Distribution Agreement

In presenting this thesis as a partial fulfillment of the requirements for a degree from Emory University, I hereby grant to Emory University and its agents the non-exclusive license to archive, make accessible, and display my thesis in whole or in part in all forms of media, now or hereafter now, including display on the World Wide Web. I understand that I may select some access restrictions as part of the online submission of this thesis. I retain all ownership rights to the copyright of the thesis. I also retain the right to use in future works (such as articles or books) all or part of this thesis.

Yixin Xu March 29, 2019

Unveiling the power of nature: Investigating the chemical composition of a medicinal plant

by

Yixin Xu

Dr. Cassandra Quave

Adviser

Department of Chemistry

Dr. Cassandra Quave

Adviser

Dr. Dennis C. Liotta

Committee Member

Dr. Emily Weinert

Committee Member

2019

Unveiling the power of nature: Investigating the chemical composition of a medicinal plant

By

Yixin Xu

Dr. Cassandra Quave

Adviser

An abstract of
a thesis submitted to the Faculty of Emory College of Arts and Sciences
of Emory University in partial fulfillment
of the requirements of the degree of
Bachelor of Sciences with Honors

Department of Chemistry

2019

Abstract

Unveiling the power of nature: Investigating the chemical composition of a medicinal plant
By Yixin Xu

The fruit part of *Carya tomentosa* has a rich history as an important medicine to many Native American tribes. The Quave Research Group has found that the methanolic extract of immature fruits of *Carya tomentosa* (CQ-640) has a half maximal effective concentration (EC_{50}) =5.5±2.2 µg/mL for growth inhibition of the Zika virus Puerto Rico strain PRVABC59 and a cytotoxicity concentration 50% (CC_{50}) >20 µg/mL. This study focuses on the development of separation and analytical methods for investigating the chemical composition of the immature fruit part of *Carya tomentosa*. An efficient fractionation process was developed using the Amberlite XAD-2 resin packing and a gradient mobile phase of deionized (DI) H_2O and methanol, generating five fractions in total and giving a total recovery yield of 93.41%. A High-Performance Liquid Chromatography (HPLC) method was developed using a 4.6*150mm Agilent ZORBAX SB-Phenyl column and a solvent system of 0.1% formic acid in H_2O and 0.1% formic acid in methanol. This method was applied to Liquid Chromatography- Mass Spectroscopy (LC-MS) runs and several putative structural matches were found under the negative mode FTMS spectrums: peak 1 detected in 640D-F1 with a retention time of 27.49 minutes has a mass to charge (m/z) ratio of 577.1379 and the generated molecular formula is $C_{30}H_{25}O_{12}^-$(Δ ppm =1.8), which matches up with the mass of procyanidin B1, B2, B3, B4, B6, B8 and proanthocyanidin B5, B7; peak 3 detected in the spectrum of 640D-F2 with a retention time of 18.81 minutes has a m/z ratio of 575.1216 and the generated molecular formula is $C_{30}H_{23}O_{12}^-$ (Δ ppm =3.6), which matches up with the mass of (+)-proanthocyanidin A2; peak 6 detected in the spectrum of 640D-F5 with a retention time of 41.61 minutes has a m/z ratio of 865.1988 and the generated molecular formula is $C_{45}H_{37}O_{18}^-$ (Δ ppm =0.27), which matches up with the mass of procyanidin C1 and C2; peak7 detected in the spectrum of 640D-F5 with a retention time of 26.27 minutes has a m/z ratio of 447.0953 and the generated molecular formula is $C_{21}H_{19}O_{11}^-$ (Δ ppm =2.0), which matches up with the mass of kaempferol 3-galactoside.

Unveiling the power of nature: Investigating the chemical composition of a medicinal plant

By

Yixin Xu

Dr. Cassandra Quave

Adviser

A thesis submitted to the Faculty of Emory College of Arts and Sciences
of Emory University in partial fulfillment
of the requirements of the degree of
Bachelor of Sciences with Honors

Department of Chemistry

2019

Acknowledgements

First, I would like to thank my primary investigator, Dr. Cassandra Quave, for two great years of mentoring. She has been not only supporting my research financially but training me in every aspect of becoming a qualified researcher. I am grateful for this precious opportunity to do cutting-edge natural product chemistry research in her lab. She has given me the tools to continue to be successful in my future graduate studies on natural-product-related research and I do not think I could have possibly asked for a better undergraduate research experience.

I would like to thank the two other members of my honor thesis committee, Dr. Dennis C. Liotta and Dr. Emily Weinert. As a big person in the field of medicinal chemistry, Dr. Dennis Liotta has given me many precious technical advices on my experimental operation and data analysis, and I look up to him as a chemist. Dr. Emily Weinert has supported me tremendously on scientific writing techniques. I could not be here today without the generous support of these two professors.

I would like to thank Dr. James Lyles from the Quave Group for being an outstanding mentor over the past two years. He has been extremely patient, inspiring and helpful in teaching me different types of wet lab techniques and the mechanism behind them. He has always been training me to become an independent and responsible researcher.

I would like to thank Dr. Akram Salam and Dr. Huaqiao Tang from the Quave Group for helping me frequently throughout my research. They have very essential influence on my research and my life, and I regard them as very good friends. I wish them all the best in their future careers beyond the Quave lab.

Finally, I would like to thank the entire Quave group for providing me with such an excellent research and learning environment.

Table of Contents

Figures and Tables

1) Introduction

1.1) Prevailing Worldwide Zika Virus Infection

Viruses are genetic entities that lie somewhere in the grey area between living and non-living states. They depend on host cells to reproduce. When found outside the host cell, viruses exist as a protein coat called capsid. When in contact with a host cell, viruses insert their genetic materials, DNA or RNA, into host cells and utilize the nucleic acids in host cells to replicate their own gene sequences. Some viruses remain dormant inside host cells for long periods, causing no obvious change in their host cells (a stage known as the lysogenic phase). But when a dormant virus is stimulated, it enters the lytic phase: new viruses are formed, self-assemble, and burst out of the host cell, killing the cell and going on to infect other cells [1]. Zika virus (ZIKV), belonging to the Flaviviridae family and the Flavivirus genus, is a positive-sense single-stranded RNA virus [2-3]. Typically, Zika virus is spread when the female Ades aegypti mosquito feeds on the blood of a person infected with ZIKV and then spread the virus to other people through bites. Common symptoms of ZIKV infection includes fever, red eyes, headache and maculopapular rash. ZIKV infection is also reported to be strongly associated with microcephaly in babies of infected pregnant women and Guillain–Barre syndrome in adults [4]. The first case of human infection was confirmed in 1964 and ZIKV got its first outbreak on the island of Yap in the Federated States of Micronesia in 2007 [5]. Then in 2013 and 2014, around 11% of the population in French Polynesia was reported to be infected by ZIKV. In 2015, ZIKV outbreak began in Brazil and then spread to other countries in South, Central and North America [6]. While in November 2016, the World Health Organization declared that the Zika virus was no longer a global emergency, it noted that the virus still represents "a highly significant and a long-term problem" since currently there is no vaccine or specific treatment against ZIKV.

1.2) Plant Second Metabolites as Source of Finding Novel Bioactive Chemicals

Second metabolites are chemical compounds or substance produced by living organisms that have a narrow species distribution[7]. They have a broad range of functions including serving as signaling molecules with other individuals of the same species, communication molecules to activate symbiotic organisms and defensive molecules against competitors and predators[8]. Many flowering plants have been well known to use second metabolites as defensive weapons against a variety of environmental threats including bacterial infection, viral infection and insects. For example, chrysanthemum plants produce pyrethrin, a monoterpenoid ester, as an insect neurotoxin [9]. Avenacin A-1, a triterpenoid saponin produced by wheats, has detergent properties and can disrupt the cell membranes of the invading wheat fungi *Gaeumannomyces graminis* [10]. Recent studies also show that heparinoid polysaccharides isolated from marine organisms can shield the initial binding sites of human herpes virus HSV-1 AND HSV-2 on the cell surface [11]. These second metabolites, though not directly involved in the normal growth and reproduction of plants, are important in securing their long-term survivability and fecundity. The work on isolating these distinctive second metabolites and identifying their therapeutic potentials are of great importance to human beings: it not only helps us rationalized the medical usages of plants in many traditional medicine records, but also serves as a good source for new drug discovery against multiple types of diseases. From 1940s to the end of 2014, 85 out of 175 (49%) anticancer small molecules approved are either natural products or directly derived therefrom [12]. Paclitaxel, sold under the brand name Taxol, is isolated from the bark of Pacific yew, *Taxus brevifolia* and has been approved in the United States for the treatment of breast, pancreatic, ovarian, Kaposi's sarcoma and non-small-cell lung cancers [13]. Artemisinin, a chemical isolated from the plant *Artemesia annua*, and its derivatives now serves as the key components in antimalarial drugs against the deadly *Plasmodium falciparum* infection [14]. In the past decades, pharmaceutical industries have shifted their focus from medicinal plants to libraries of synthetic compounds as drug discovery source. However, at the same time there has been a declining trend in the number of new drugs reaching the market, raising renewed scientific interest in drug

discovery from natural sources, despite of its known challenges. Up to date, only a small fraction of the known plant species on earth (~450,000 spp.) have been investigated for their pharmacological potential and currently less than 10% of this total number are exploited by humans for medicinal purposes [15]. Additionally, records of applying natural-product-derived chemicals in antiviral treatment remain limited. Here we decide to address the issue of ZIKV infection through an ethnobotanical approach to drug discovery.

1.3) Ethnobotanical Approach to Drug Discovery against ZIKV Infection

Plant species on earth have been exploited by humans for medicinal purposes for hundreds of years. Reviewing the traditionally medicinal uses of plants in different regions worldwide serves as a good starting point to investigate the novel therapeutic potent of plants that have barely been investigated before.

Carya tomentosa (Poir.) Nutt, Juglandaceae, commonly known as the mockernut hickory, is investigated here for its therapeutic potential. *Carya tomentosa* has also been reported under the following synonyms, which are no longer used as accepted names nowadays: *Carya alba* (L.) K. Koch, *Hicorius alba* Britton, and *Juglans tomentosa* Poir. The fruit part of *Carya tomentosa* (Figure 1) has a rich history as an important medicine to a number of Native American tribes. The Cherokee used it as an analgesic, cold remedy, dermatological aid, diaphoretic, emetic, gastrointestinal aid, for poliomyelitis pain, and for mouth sores. The Delaware used it as a tonic and for “female disorders” [16].

Figure 1. Fruits of *Carya tomentosa*

The initial hit for antiviral activity against ZIKV was detected in the methanolic extract of the immature fruits of *Carya tomentosa* collected on Emory's campus.

1.4) Project Aims and Research Questions

Since the initial hit for anti-ZIKV activity has been detected in the methanolic crude extract of the immature fruits of *Carya tomentosa*, the long-term goal of this research is to investigate the chemical constituents in this plant that are responsible for the overall anti-ZIKV activity of its immature fruits.

As one important part of this research, this project aims at developing the chemical separation methodology for the purpose of investigating the chemical composition of the *Carya tomentosa* immature fruits and identifying anti-ZIKV bioactive constituents. The project includes development of methods all the way from fractionation, high-performance liquid chromatography (HPLC) method development, Liquid Chromatography- Mass Spectroscopy method development to the putative structural analysis.

2) Literature Review

2.1) Chemical Profile Investigation on *Carya tomentosa* and its Relative Species

While chemical composition of *Carya tomentosa* has not been extensively studied, we have a relatively clear picture of the chemical profile of *Carya illinoensis*, another species from the same genus, which is also commonly known as pecan. The moisture, protein, lipid and total soluble sugars contents in pecan range from 2.1% to 6.4%, 6% to 11.3%, 65.9% to 78% and 3.3 to 5.3% respectively. Pecans are low in saturated fats but rich in monounsaturated fatty acids, primarily oleic acid (52.52-74.09%) and polyunsaturated fatty acids, predominantly linoleic acid (17.69-37.52%). Pecans are also rich in phenolics notably, flavonoid glycosides and aglycones, galloylated glycosides and condensed tannins [17]. It is reported that the acetonic extracts of the *Carya illinoensis* kernel and shell parts collected from the state of Chihuahua, Mexico contain high contents of gallic acid, ellagic acid (phenolic acids), rutin (flavonoids), catechin and epicatechin (condensed tannin) [18]. Pecans are also good source of tocopherols, which are forms of lipid-soluble vitamin E, and exist as four different isomers: alpha, beta, gamma and delta. Pecans have unusually high content of gamma-tocopherol, which is around 25mg of gamma-tocopherol in every 100 grams of pecan kernels and shells [19].

2.2) Bioactivity of Phytochemicals Found in Related Species of *Carya tomentosa*

Multiple studies demonstrate the antimicrobial activity of pecan nutshell against Gram-positive bacteria such as *L. monocytogenes, S. aureus, B. cereus* and *V. parahaemolyticus* and Gram-negative bacteria such as *S.* Enteritidis, *A. hydrophila* and *P. aeruginosa*. The antimicrobial activities detected in the crude extract of *Carya illinoensis* kernels and shells are consistent with the high contents of phenolic acids and condensed tannin in its chemical profile. Gallic and ferulic acids are electrophilic products and have been previously shown to significantly interact with the bacterial surface component, destabilizing cell cytoplasmic membrane of pathogenic bacteria such as E. *coli, L. monocytogenes, P. aeruginosa* and *S. aureus.* Six pecan cultivars were analyzed for their antioxidant capacity (AC) and it was found that

phenolic compounds with high antioxidant capacity are in kernels and shells [20]. These Phenolic acids (gallic acid and ellagic acid), flavonoids (rutin), and tannins (catechins and epicatechins) were identified by HPLC-DAD and were thought to be partially responsible for the antimicrobial activity. The gamma-tocopherol present in the kernel and shell of pecans has been suggested to be able to detoxify reactive nitrogen oxide species and thus reduce inflammation in human bodies. Gamma-tocopherol has also been observed to act as a better antioxidant in vivo than alpha-tocopherol [19]. Thus, the presence of high contents of gamma-tocopherol in the kernel and shell parts also contributes to the overall antioxidant properties of *Carya illinoensis.*

The chemical profile of *Carya illinoensis* nuts and shells along with its reported antioxidant and antimicrobial activity serve as a good reference for our investigation into the bioactive constituents from *Carya tomentosa*.

2.3) Biological Assessment of the Anti-ZIKV Potential of *Carya tomentosa*

The Quave Research Group screened approximately 10% of the Quave Natural Product Library (QNPL) for growth inhibitory activity against ZIKV. Vero cells were exposed to 20 µg/mL extract immediately following infection with the ZIKV (MOI=0.01) Puerto Rico strain PRVABC59 (NCBI accession KU501215). Cell cytopathic effect (CPE) MTS assay (Promega) was measured 4 days after treatment to determine replication inhibition potency. The methanolic extract of immature fruits of *Carya tomentosa* (CQ-640) was identified with a half maximal effective concentration (EC_{50}) $= 5.5 \pm 2.2$ µg/mL against ZIKV Puerto Rico strain PRVABC59, indicating that the extract with a concentration of 5.5 ± 2.2 µg/mL could induce a viral replication inhibition response halfway between the baseline and maximum. Experimental data also indicated that the extract has a cytotoxicity concentration 50% (CC_{50}) $>$ $20\mu g/mL$, which is the concentration of the extract to kill half of the uninfected cells.

Extract CQ-640 was then partitioned via a modified Kupchan scheme [21]. The dried CQ-640 extract was resuspended in water at 1g: 33mL and underwent sequential liquid-liquid partitioning three times each

with an equal volume of hexane, ethyl acetate, and normal butanol (n-butanol). The organic partitions were dried over Na_2SO_4 and filtered. Each partition was concentrated in vacuum at 40 °C, suspended in DI H_2O, lyophilized, ground into powder and stored at -20 °C. Resultant partitions were hexane partition (640B), ethyl acetate partition (640C). butanol partition (640D) and aqueous partition (640E).

3) Materials and Methods

3.1) Experimental Overview

A series of chemical analysis and biological assays were performed to investigate the bioactivity of the immature fruit extracts of *Carya tomentosa* (Figure 2). Experiments focused on the development of an appropriate fractionation method for purifying crude extracts and the identification of compounds with anti-ZIKV activity.

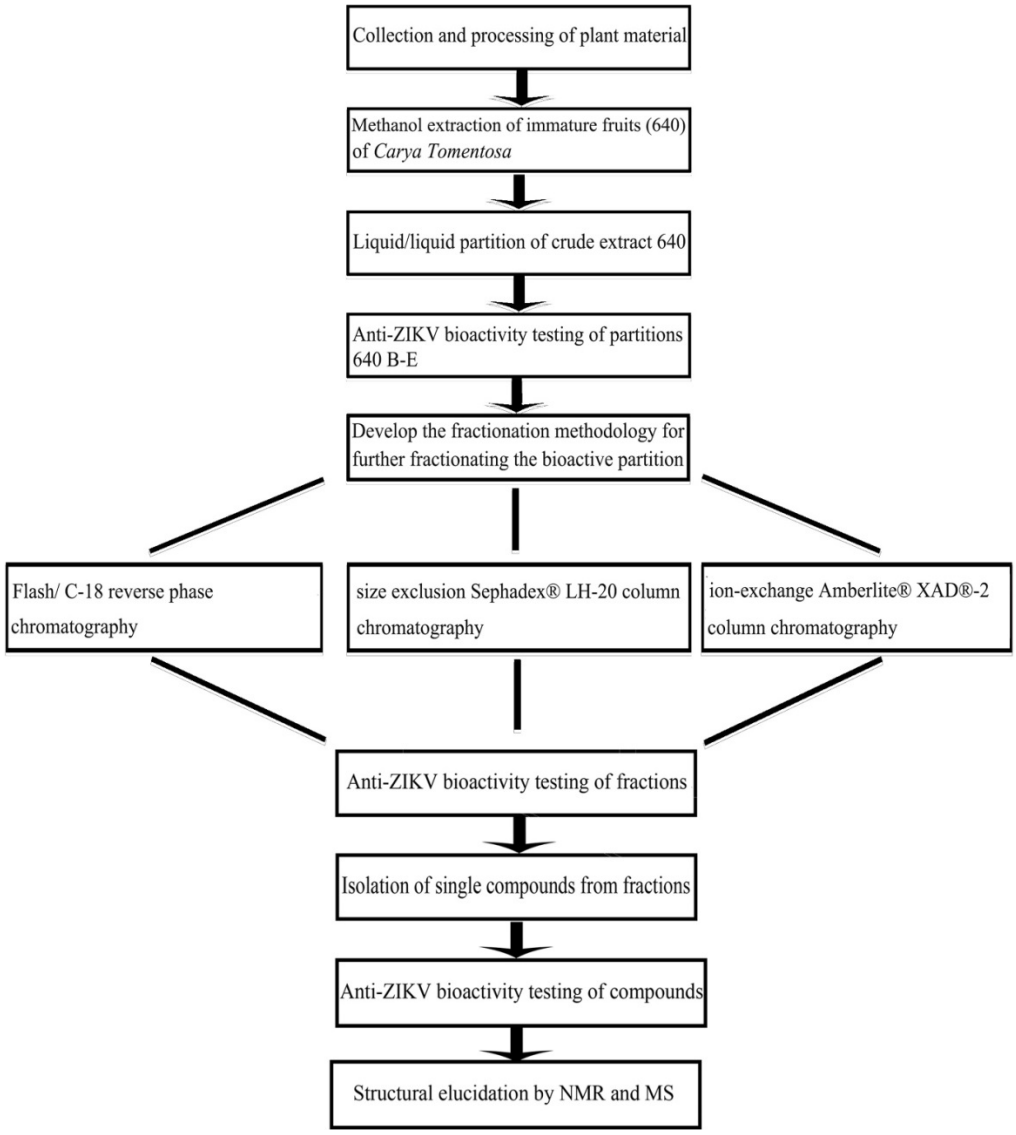

Figure 2. Experimental Procedure Overview

3.1.1) Extraction

For each trial of maceration, 50g of dried *Carya tomentosa* immature fruits were blended with 500 mL methanol (MeOH) and sonicated for 20 minutes. The extraction was then vacuum filtered and the remaining plant materials were macerated with 500 mL MeOH again following the same procedure. This process was repeated for a total of three times. Filtered extracts were combined and concentrated by rotary evaporation at reduced pressure. The concentrated extracts were resuspended in deionized water, lyophilized and stored at -20°C. The extract was labeled as 640. A total of 6 trials of extraction were conducted on March 6th, 2018 and March 12th, 2018 and all processed CQ-640 extracts were recombined and stored at -20°C.

3.1.2) Partition

A modified Kupchan partitioning scheme in succession with hexane, ethyl acetate and butanol was used in the separation of extracts CQ-640. All ACS (American Chemical Society) grade solvents were obtained from Fisher Chemical. For each partition, approximately 16 g of processed Extract CQ-640 were dissolved in 500 mL of 20% MeOH/ DI H_2O solution. The solution was transferred into a 1L separatory funnel and mixed with 500mL of hexanes. The organic layer was removed, filtered through anhydrous sodium sulfate (Na_2SO_4) and stored in a 3L jar labeled as “640B”. The aqueous solution was mixed with 500 mL hexanes two more times following the same procedure. This process was repeated with ethyl acetate and n-butanol. The ethyl acetate solution was labeled as “640C” and the n-butanol solution was labeled as “640D”. The remaining MeOH/H2O solution was filtered through filter paper and labeled as “640E” (Table 1). Each partition was then rotary evaporated, re-dissolved in DI H2O, lyophilized and stored at -20°C.

Table 1. Summary of extraction and partition scheme

Extract Name	Plant Part	Description
640	Immature fruits	Crude extract
640B		Hexane partition
640C		Ethyl acetate partition
640D		n-Butanol partitin
640E		Aqueous partition

3.2) Fractionation Method Development

3.2.1) Fractionation through Sephadex LH-20 Column Chromatography

Sephadex® LH-20 resins are hydroxypropylated, cross-linked dextran structures in the form of porous beads. Thus, they have both hydrophilic and lipophilic characters. Depending on the mobile system used, Sephadex® LH-20 chromatography can separate molecules either based on their affinity to the resins or based on their molecular sizes [22]. Sephadex® LH-20 resins have been used to separate a wide range of natural products in either an aqueous or non-aqueous solvent system, including feruloylated arabinoxylan oligosaccharides from cereal grain intermediate wheat [23], pyrimidine diterpenes from sea sponge *Agelas axifera* [24] and (-)-epicatechins and proanthocyanidins from cocoa beans [25].

In this experiment, Sephadex® LH-20 resins were used mainly for affinity chromatography. 21.74 g Sephadex® LH-20 was measured out in a 500mL beaker. 95% ethanol (EtOH) was added into the beaker and mixed with Sephadex® LH-20 to make a slurry. A small amount of 95% EtOH solution was first added into a 45cmx1cm glass column. Then the Sephadex® LH-20 / H2O slurry was then added into the column. As soon as the slurry touched the 95% EtOH solution in the column, the stopcock was open to enable compact packing of Sephadex® LH-20. After adding all the slurry into the column, two column volumes of 95% EtOH solution were added from the top of the column and allowed to pass through the column. 1.00 g of 640D extract was dissolved in 5 mL of 95% EtOH solution and sonicated for 5 minutes. The 640D solution was loaded onto the column. After the Sephadex® LH-20 packing absorbed all the

640D solution, a total of 7 column volumes of 95% EtOH solution were added onto the column. The first 30 mL of eluate was collected and labeled as F1. Every following 10 mL of eluate was collected and labeled as F2, F3, F4……. A total of 17 fractions (F1~F17) were collected using 95% EtOH as the mobile phase. Then 6 column volumes of 1:1 acetone: 95% EtOH solution were added onto the column. Every 10 mL of eluate was collected as one fraction and labeled following the order from F18 to F23. To speed up the fractionation process, every 20 mL of eluate was collected as one fraction from F24 to F33. A total of 16 fractions were collected using 1:1 acetone: 95% EtOH solution as the mobile phase. Finally, two column volumes of acetone were added onto the column. The last 50 mL of eluate was collected and labeled as F34. Each fraction was then vacuum filtered and dried down completely using the bar evaporator. The percent yield of each fraction was calculated based on the equation

$$\%yield = \frac{mass\ of\ the\ fraction}{1.00g\ of\ 640\ crude\ extract} * 100 \quad (1)$$

Around 2 mg of each fraction was then dissolved in 200 μL of HPLC grade MeOH to make a solution of 10mg/mL. These solutions were centrifuged at 5000 RPI for 15 minutes and the supernatants were transferred into HPLC vials. A 4.6 x 250 mm Agilent Eclipse XDB C-18 column was used for HPLC analysis. The following solvent system and gradient were applied (Table 2):

Table 2. HPLC method for 640D samples fractionated by LH-20 column on a 4.6 X 250 mm Agilent Eclipse XDB C-18 column

Time (min)	A (%)	B (%)	Flow Rate (mL/min)
0.00	98.0	2.0	1.00
5.00	98.0	2.0	1.00
60.00	2.0	98.0	1.00
70.00	2.0	98.0	1.00
70.10	98.0	2.0	1.00
80.00	98.0	2.0	1.00

3.2.2) Fractionation through Amberlite® XAD®-2 Column Chromatography

Amberlite® XAD®-2, as another type of resin, is a hydrophobic copolymer of styrene-divinylbenzene resin that absorbs organic compounds according to aromaticity and size of hydrophobic groups. Amberlite® XAD®-2 resin has been widely used in chromatography to remove phenols and aromatic compounds of molecular weight up to 20,000 g/mol. Since it was indicated that the anti-ZIKV bioactivity of 640D crude extracts was lost after Flash chromatography and C-18 reversed phase chromatography, it was suspected that the bioactive constituents in 640 crude extracts have aromatic and polyphenolic characteristics. Hence, Amberlite® XAD®-2 resin was chosen to fractionate 640D crude extracts.

To prepare the column, XAD-2 resin was mixed with DI H_2O to make a slurry. Then the slurry was added into a 130cmx1.5cm glass column. After the column was ¾ filled, DI H_2O was added to cover the top of the column. The column was then backwashed with DI H_2O to remove any bubbles and resin debris. After backwashing, the column was washed with a hydrochloric acid solution (pH=2) till the pH value of the eluate was the same as that of the eluent. Finally, the column was washed again with DI H_2O till the pH of the eluate was approximately neutral. The sample was prepared by dissolving 2.33 grams of 640D powder in DI H_2O and was loaded onto the packed column. Three column volumes of DI H_2O were used as the first mobile phase, three column volumes of 1:1 MeOH: H_2O solution as the second mobile phase and finally three column volumes of MeOH as the third mobile phase. Fractions were collected based on the solvent of the eluate. The collection scheme is shown as following: first column volume as F0→next three column volumes as F1→next one column volume as F2→ next three column volumes as F3→ next one column volume as F4→ final three column volumes as F5. Each fraction was then vacuum filtered, dried down completely using the bar evaporator, wrapped with tin foil and preserved in the -20°C freezer. The percent yield of each fraction was calculated based on equation (1).

Thin Layer Chromatography (TLC), with silica as the solid phase, was used to check the chemical composition of each fraction before the HPLC analysis. Different mobile phases were and 3:4 MeOH: Dichloromethane with 4% formic acid was determined to be the most appropriate mobile phase. Around 2

mg of each fraction was then dissolved in 200 μL of HPLC grade MeOH to make a solution of 10mg/mL. These solutions were centrifuged at 5000 RPI for 15 minutes and the supernatants were transferred into HPLC vials. A 4.6x50mm Agilent Poroshell 120 EC-C18 column was used for HPLC analysis. The following solvent system, gradient and injection volume were applied (Table 3):

Table 3. HPLC method for 640D samples fractionated by XAD-2 resin column on a 4.6x50mm Agilent Poroshell 120 EC-C18 column

Solvent System	Sample injection volume (uL)	Time (min)	A (%)	B (%)	Flow Rate (mL/min)
A=0.3%formic acid in H_2O, B= methanol	10	4.50	98.0	2.0	1.00
		16.50	0.0	100.0	1.00
		21.00	0.0	100.0	1.00
		21.10	98.0	2.0	1.00
		26.00	98.0	2.0	1.00

3. 3) HPLC Method Development

In order to acquire chromatograms on HPLC with well separated and resolved peaks, the HPLC method was modified by changing the column packing, solvent system and solvent gradient. First, two alternative column packings were tried other than originally used Agilent Poroshell 120 EC-C18 column: a 3.5um, 4.6*150mm Agilent ZORBAX SB-Phenyl column and a 2.6um, 2.1*50mm Kinentex HILIC column. The separation principles of the Agilent ZORBAX SB-Phenyl are hydrophobic interaction and π -π interaction which is not present in the C-18 reversed phase column. Hence, compounds with different degree of aromaticity could be better separated out by the phenyl column than the C-18 column. The Agilent ZORBAX SB-Phenyl column was chosen for testing due to the suspected high contents of aromaticity in the fractionation samples. The following solvent system and gradient were applied to the 3.5um, 4.6*150mm Agilent ZORBAX SB-Phenyl column (Table 4, Figure 3):

Table 4. HPLC method for 640D samples fractionated by XAD-2 resin column on a 4.6*150mm Agilent ZORBAX SB-Phenyl column

Solvent System	Sample injection volume (uL)	Time (min)	A (%)	B (%)	Flow Rate (mL/min)
A=0.1%formic acid in H_2 O, B= 0.1% formic acid in acetonitrile	10	13.50	98.0	2.0	1.00
		36.50	0.0	100.0	1.00
		58.50	0.0	100.0	1.00
		58.60	98.0	2.0	1.00
		72.06	98.0	2.0	1.00

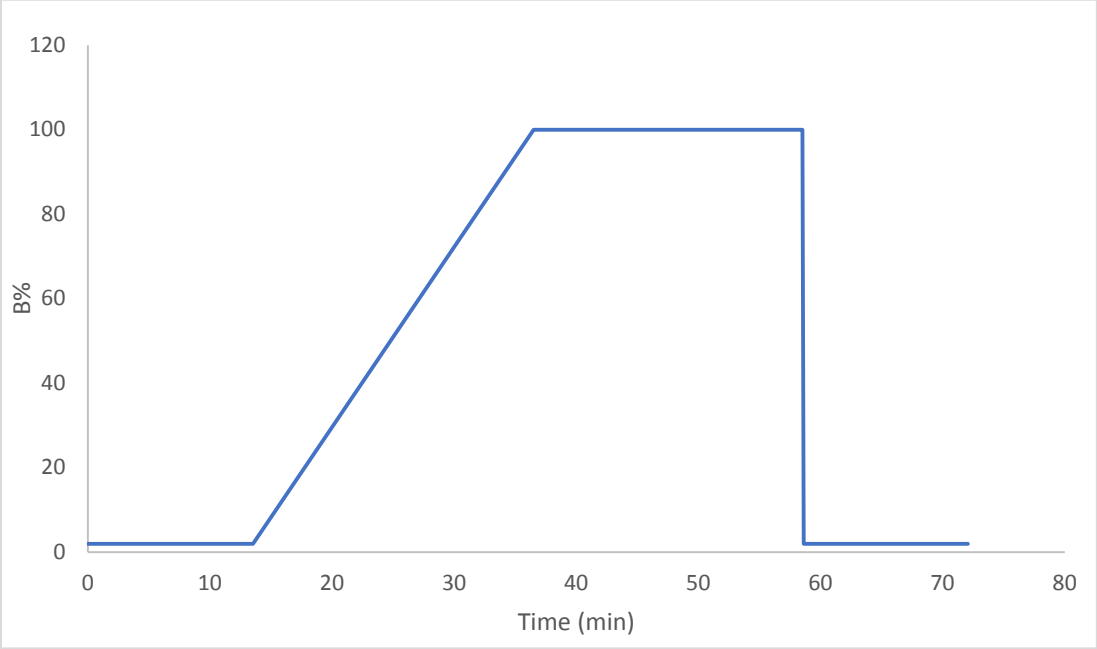

Figure 3. Solvent gradient diagram of the HPLC method shown in Table 4.

The separation principle of the Kinentex HILIC column was the hydrophilic interaction where analytes elute in the order of increasing polarity. This column was chosen due to the suspected phenolic characteristics in the fractionation samples. The following solvent system and gradient were applied to the 2.6um, 2.1*50mm Kinentex HILIC column (Table 5, Figure 4):

Table 5. HPLC method for 640D samples fractionated by XAD-2 resin column on a 2.1*50mm Kinentex HILIC column

Solvent System	Sample injection volume (uL)	Time (min)	A (%)	B (%)	Flow Rate (mL/min)
A=0.1%formic acid in H_2O, B= 0.1% formic acid in acetonitrile	10	12.00	10.0	90.0	1.00
		17.20	50.0	50.0	1.00
		22.40	50.0	50.0	1.00
		58.60	10.0	90.0	1.00
		72.06	10.0	90.0	1.00

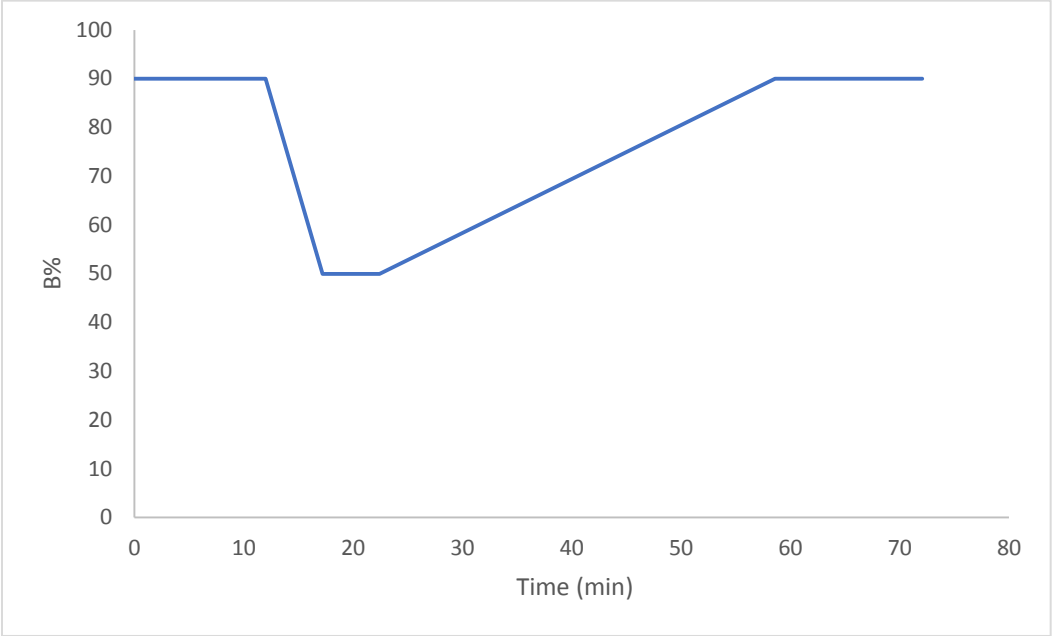

Figure 4. Solvent gradient diagram of the HPLC method shown in Table 5.

Two solvent systems were tried out for better separation of peaks. One is composed of A) 0.1% formic acid in H_2O and B) 0.1% formic acid in methanol and the other is composed of A) 0.1% formic acid in H_2O and B) 0.1% formic acid in acetonitrile.

Multiple solvent gradients were tested based on the quality of peak separation. The original gradient applied in Table 4 was adjusted to be more gradual and this adjusted gradient was shown in Table 6 and Figure 5.

Table 6. Adjusted HPLC method for 640D samples fractionated by XAD-2 resin column on a 4.6*150mm Agilent ZORBAX SB-Phenyl column

Solvent System	Sample injection volume (uL)	Time (min)	A (%)	B (%)	Flow Rate (mL/min)
A=0.1%formic acid in H_2O, B= 0.1% formic acid in methanol	10	13.50	98.0	2.0	1.00
		20.00	70.0	30.0	1.00
		31.00	45.0	55.0	1.00
		42.00	0.0	100.0	1.00
		64.00	0.0	100.0	1.00
		64.01	98.0	2.0	1.00
		78.00	98.0	2.0	1.00

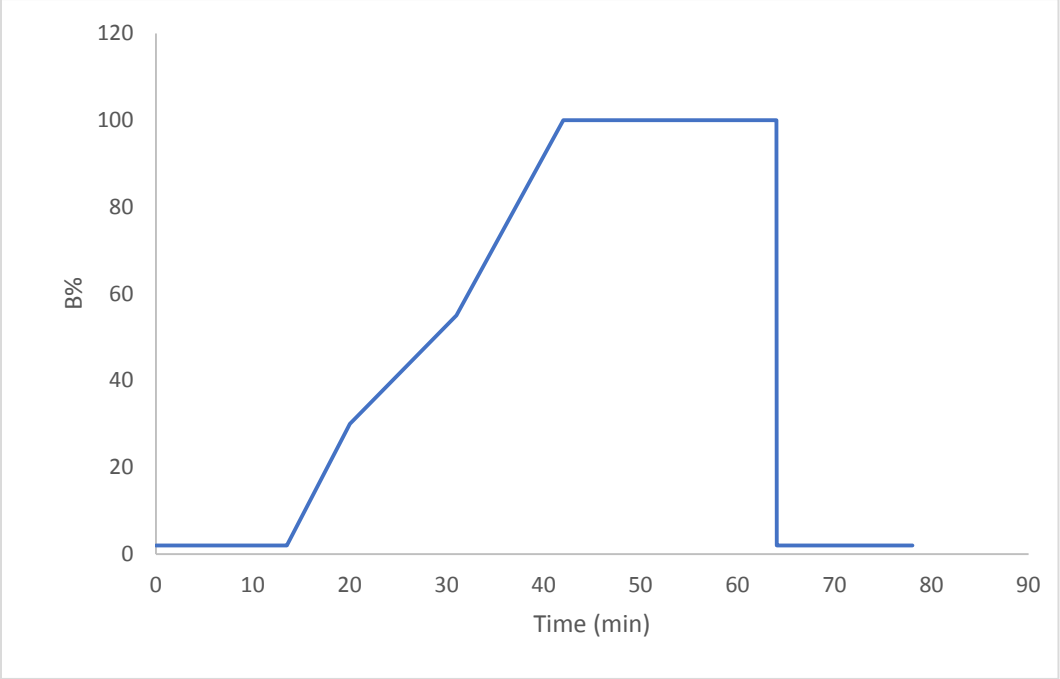

Figure 5. Solvent gradient diagram of the HPLC method shown in Table 6.

The isocratic solvent gradient was also tested since the isocratic gradient theoretically would give the best separation of peaks for an established solvent system. The isocratic method was shown below in Table 7 and Figure 6.

Table 7. 15% MeOH isocratic HPLC method for 640D samples fractionated by XAD-2 resin column on a 4.6*150mm Agilent ZORBAX SB-Phenyl column

Solvent System	Sample injection volume (uL)	Time (min)	A (%)	B (%)	Flow Rate (mL/min)
A=0.1%formic acid in H_2O, B= 0.1% formic acid in methanol	10	0.00	85.0	15.0	1.00
		60.00	85.0	15.0	1.00
		61.00	0.0	100.0	1.00
		76.00	0.0	100.0	1.00
		77.00	85.0	15.0	1.00
		92.00	85.0	15.0	1.00

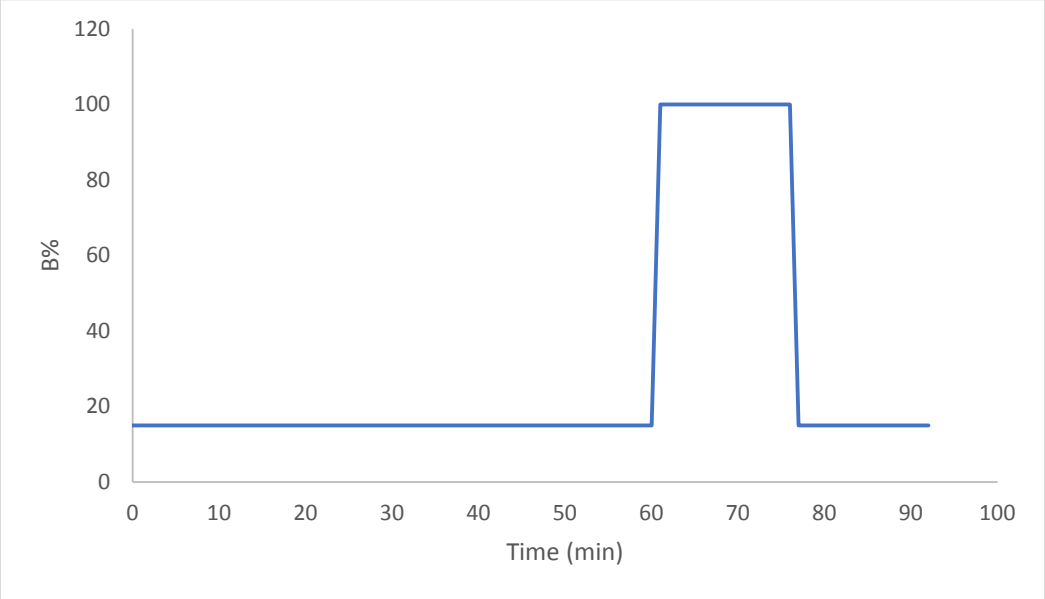

Figure 6. Solvent gradient diagram of the HPLC method shown in Table 7.

3.4) LC-MS Method Development

The column, solvent systems and solvent gradients with which best separation of peaks were achieved on the chromatogram were selected and used in the following Liquid Chromatography- Mass Spectroscopy process. All the mass spectrums acquired by Fourier-Transform Mass Spectroscopy (FTMS) were analyzed with Thermo Xcalibur Qual Browser.

4) Results and Discussion

4.1) Fractionation Method Development Results

The mass of each fraction and the percent yield data acquired from fractionation by Sephadex LH-20 column chromatography are listed in Table 8.

Table 8. Mass and % yield data of fractionation by Sephadex® LH-20 column chromatography

Mobile Phase	Fraction Number (F#)	Mass (mg)	% yield
95% EtOH	640D-F1	0.76	0.076
95% EtOH	640D-F2	3.72	0.372
95% EtOH	640D-F3	68.32	6.832
95% EtOH	640D-F4	32.44	3.244
95% EtOH	640D-F5	4.92	0.492
95% EtOH	640D-F6	3.74	0.374
95% EtOH	640D-F7	3.91	0.391
95% EtOH	640D-F8	2.58	0.258
95% EtOH	640D-F9	4.88	0.488
95% EtOH	640D-F10	6.97	0.697
95% EtOH	640D-F11	5.16	0.516
95% EtOH	640D-F12	9.79	0.979
95% EtOH	640D-F13	11.46	1.146
95% EtOH	640D-F14	4.62	0.462
95% EtOH	640D-F15	2.97	0.297
95% EtOH	640D-F16	1.81	0.181
1:1 acetone: 95% EtOH	640D-F17	3.15	0.315
1:1 acetone: 95% EtOH	640D-F18	9.23	0.923
1:1 acetone: 95% EtOH	640D-F19	2.79	0.279
1:1 acetone: 95% EtOH	640D-F20	92.2	9.22
1:1 acetone: 95% EtOH	640D-F21	163.09	16.309
1:1 acetone: 95% EtOH	640D-F22	119.85	11.985
1:1 acetone: 95% EtOH	640D-F23	52.3	5.23
1:1 acetone: 95% EtOH	640D-F24	64	6.4
1:1 acetone: 95% EtOH	640D-F25	42.04	4.204
1:1 acetone: 95% EtOH	640D-F26	27.23	2.723
1:1 acetone: 95% EtOH	640D-F27	19.59	1.959
1:1 acetone: 95% EtOH	640D-F28	16.23	1.623
1:1 acetone: 95% EtOH	640D-F29	14.32	1.432
1:1 acetone: 95% EtOH	640D-F30	7.94	0.794
1:1 acetone: 95% EtOH	640D-F31	7.34	0.734
1:1 acetone: 95% EtOH	640D-F32	5.49	0.549
1:1 acetone: 95% EtOH	640D-F33	3.07	0.307
acetone	640D-F34	1.7	0.17

The total recovery rate was calculated to be 81.952%, indicating an unignorable amount of sample loss. The stacked HPLC chromatograms for parent samples (CQ-640 and 640D) and each fraction acquired at wavelength= 217nm by Sephadex LH-20 column chromatography are shown below in Figure 7.

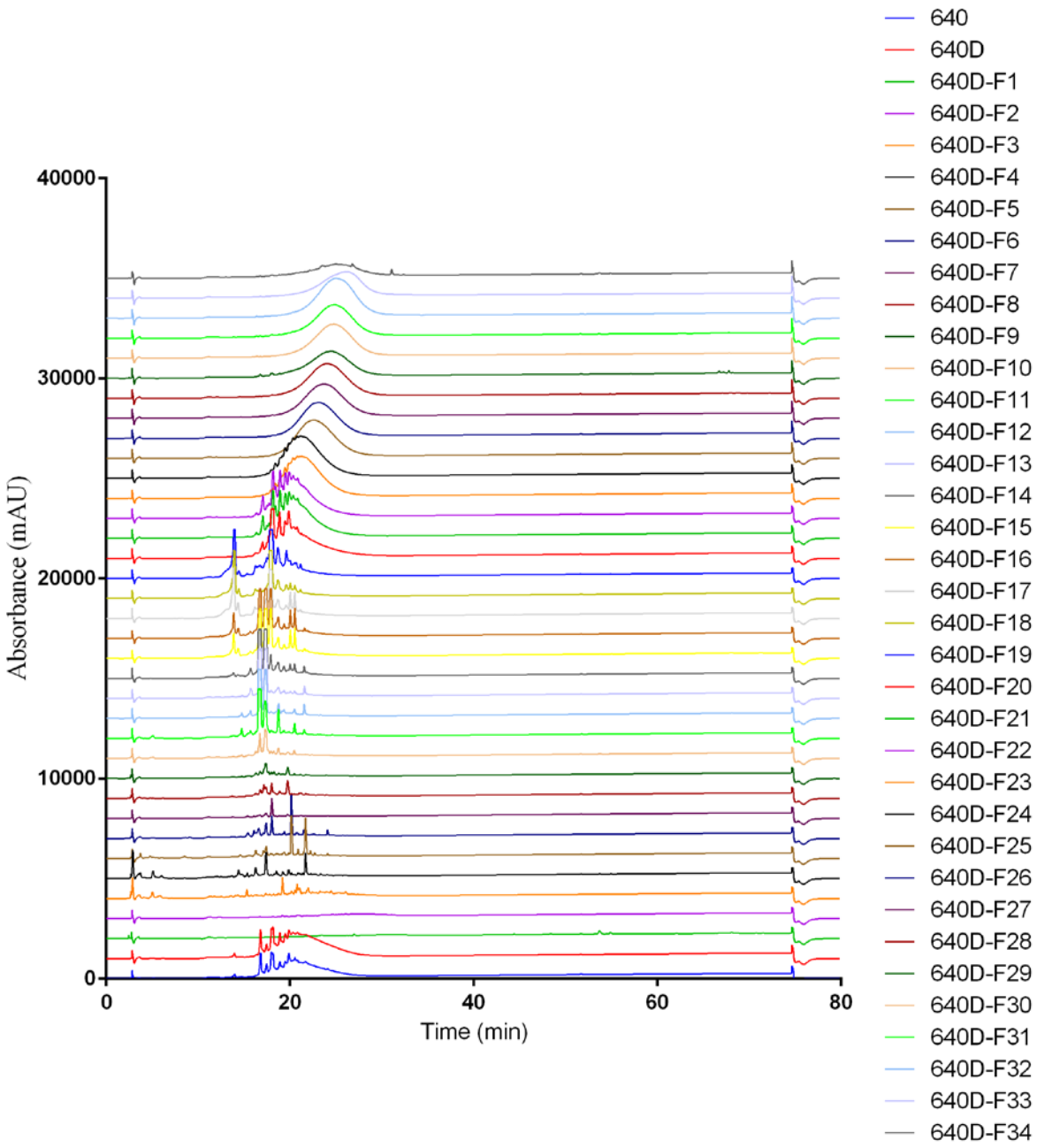

Figure 7. Stacked HPLC chromatograms of CQ-640 parent samples and fractions acquired at λ =217nm by Sephadex® LH-20 column chromatography

It was observed that most peaks in the chromatogram are retained around 15 to 30 minutes. Besides, a single peak with high absorbance was observed to be retained around 5 minutes in every fraction. Both phenomena indicate a poor distinction in chemical composition among fractions. Additionally, the relatively low recovery rate of 81.952% further supports the idea that size-exclusion Sephadex LH-20 column might not be an appropriate chromatography method for fractionating 640D.

The mass of each fraction and the percent yield data acquired from fractionation by Amberlite XAD-2 column chromatography is listed in Table 9.

Table 9. Mass and % yield data of fractionation by Amberlite® XAD®-2 column chromatography

Mobile phase	Fraction #	mass (g)	% yield
H2O(wash)	640D-XAD-F0	0.0874	3.7511
H2O	640D-XAD-F1	1.9478	83.6
H2O/MeOH	640D-XAD-F2	0.0265	1.137
H2O/MeOH	640D-XAD-F3	0.0901	3.867
H2O/MeOH	640D-XAD-F4	0.0128	0.549
MeOH	640D-XAD-F5	0.0118	0.50644

The total recovery rate was calculated to be 93.41%. The appearance of each fraction acquired by Amberlite XAD-2 column chromatography was shown below in Figure 10~14:

Figure 10. Appearance of 640D-XAD-F1: dark brown red chunk

Figure 11. Appearance of 640D-XAD-F2: brown powder

Figure 12. Appearance of 640D-XAD-F3: brown powder

Figure 13: Appearance of 640D-XAD-F4: yellow-green powder with distinctive odor

Figure 14: Appearance of 640D-XAD-F5: orange-yellow powder with distinctive odor

The TLC outcome for each fraction acquired by Amberlite XAD-2 column chromatography was shown in Figure 15.

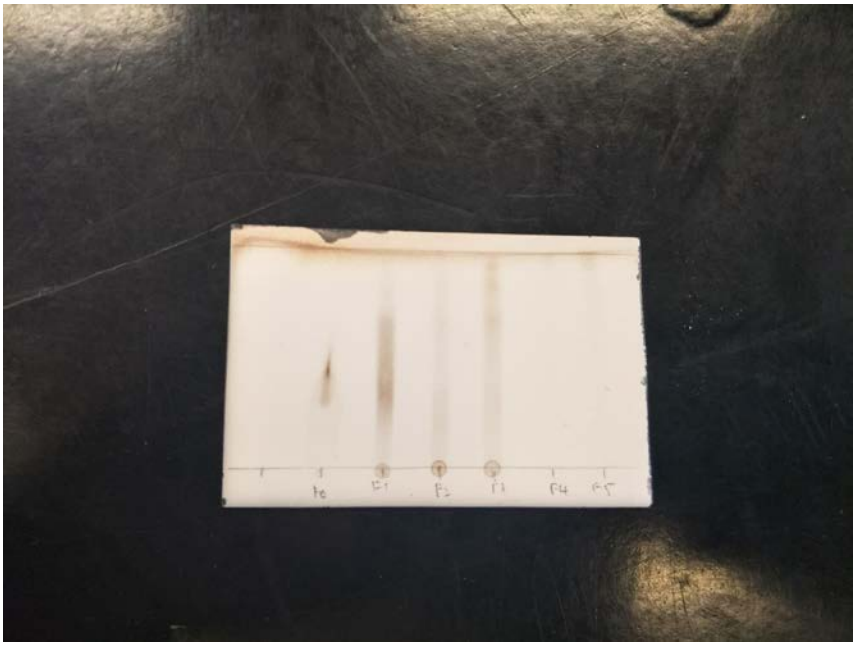

Figure 15. TLC outcome of each fraction collected using Amberlite® XAD®-2 column chromatography

The acquired HPLC chromatogram at λ=217nm for each fraction acquired by Amberlite XAD-2 column chromatography and its parent samples (640 and 640D) are shown below in Figure 16.

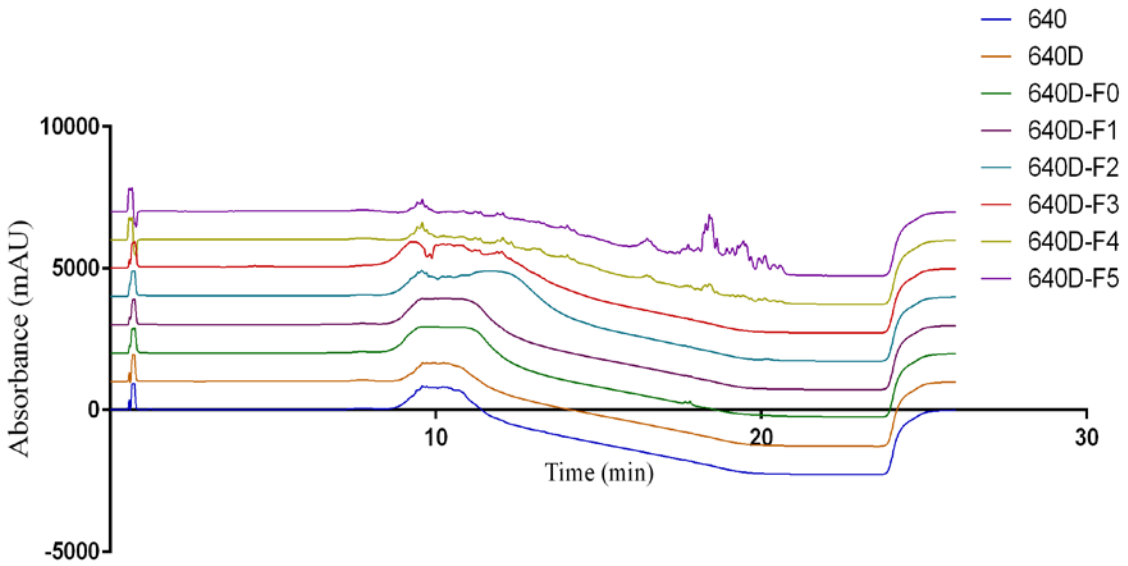

Figure 16. Stacked chromatograms of CQ-640 parent samples and fractions acquired at λ =217nm by Amberlite® XAD®-2 column chromatography

It was observed that majority of the peaks are retained from 9 to 13 minutes for 640D-F0, F1, F2 and F3. Multiple peaks are retained from 9 to 21 minutes for 640D-F4. Similar patterns are observed for F5 but with higher absorbance. Comparison between these chromatograms indicates more distinctive chemical compositions among different fractions. Additionally, the difference in color and odor among fractions, the TLC result and the relatively high recovery rate of 93.41% further support the idea that Amberlite® XAD®-2 column serves as an appropriate chromatography method for fractionating 640D.

4.2) HPLC Method Development Results

With the originally Agilent Poroshell 120 EC-C18 column being used, a single peak eluting around 2 min is repeatedly observed on the chromatogram of each XAD fraction (Figure 12). This single peak with high absorbance indicated that some chemicals in the fraction disfavor the solid phase condition so much that they eluted all at once when the mobile phase went through the column. Thus, it is highly possible that this peak did not represent a single compound but rather a mixture of different chemicals. Therefore, an alternative HPLC method was developed.

The following stacked chromatograms (Figure 17) were acquired on each XAD fractionated fraction at λ =217nm using the 3.5um, 4.6*150mm Agilent ZORBAX SB-Phenyl column and the method shown in Table 4:

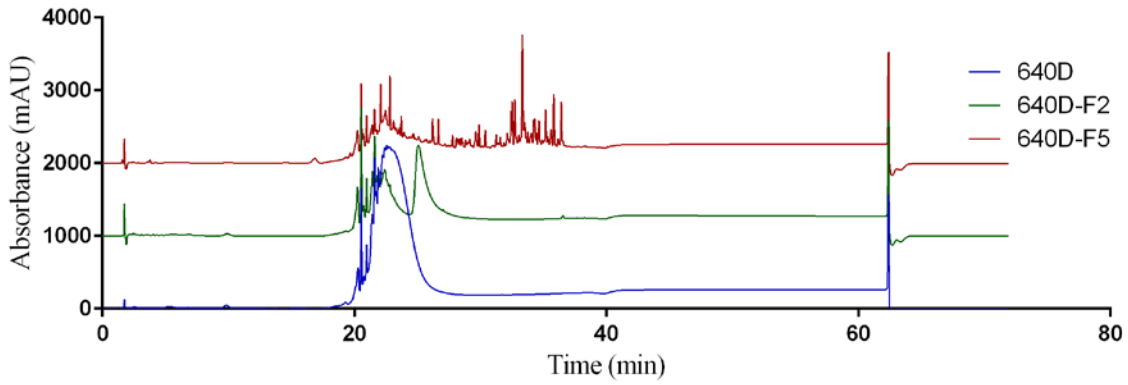

Figure 17. Stacked HPLC chromatograms of 640D, 640D-F2 and 640D-F5 at λ =217nm acquired by Agilent ZORBAX SB-Phenyl column and the method shown in Table 4.

And the following stacked chromatograms (Figure 18) were acquired on each XAD fractionated fraction at λ =217nm using the Kinetex 2.6um, 2.1*50mm HILIC column and the method shown in Table 5:

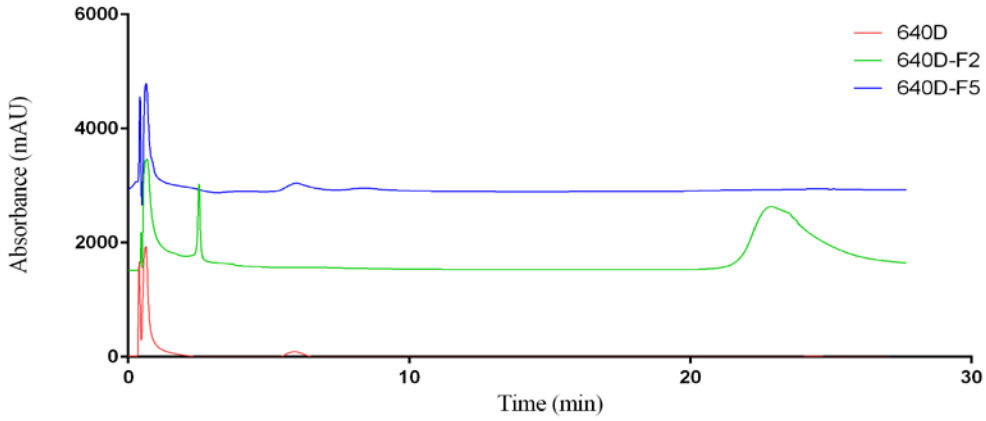

Figure 18. HPLC chromatograms of 640D, 640D-F2 and 640D-F5 at λ =217nm acquired by Kinetex 2.1*50mm HILIC column and the method shown in Table 5.

Figure 18 reveals that with the Kinetex HILIC column, majority of the peaks elute in less than one minute, indicating that most constituents in the 640D extracts are not compatible with the column. Figure 17

indicates a much better separation of peaks compared to Figure 18. Thus, it was concluded that the ZORBAX SB-Phenyl column was more compatible with the XAD fractionated samples and was selected for use in the following HPLC method development.

Between the two solvent systems, the H_2O/ methanol system gives a slightly better separation of peaks on the chromatogram of 640D and was thus applied in the following HPLC method optimization process.

The stacked chromatograms of 640D, 640D-F2 and F5 acquired at wavelength= 217nm by using the method shown in Table 6 was shown in Figure 19.

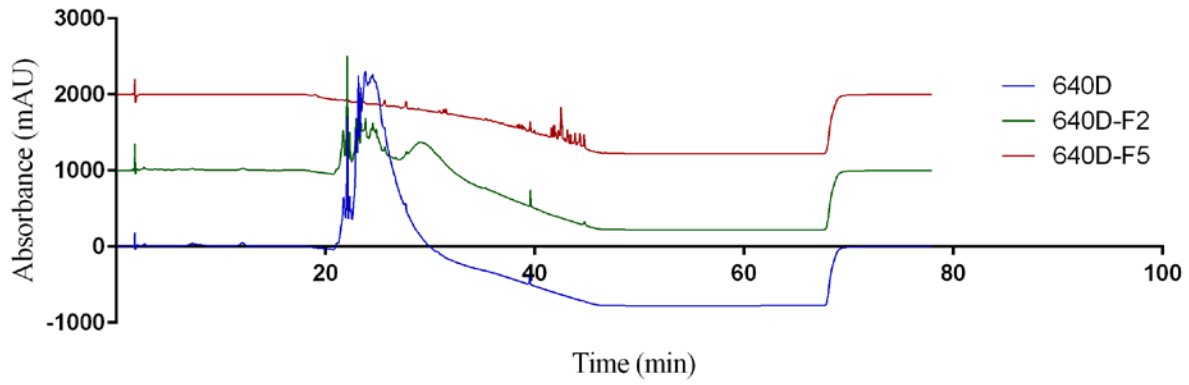

Figure 19. Stacked HPLC chromatograms of 640D, 640D-F2 and 640D-F5 at λ =217nm acquired by Agilent ZORBAX SB-Phenyl column and the method shown in Table 6.

The negative absorbance present in Figure 21 is very possibly caused by the fact that the absorbance of the analytes is lower than that of the mobile phase. The sudden increase in percentage of methanol in the solvent after 20 min is in correspondence with the time at which negative absorbance starts to occur. Comparison between Figure 17 and Figure 19 also reveals that Figure 19 has a better separation of peaks for 640D-F2 and 640D. Thus, the adjusted solvent gradient shown in Table 6 was used for HPLC method optimization.

Since separation of peaks appeared to be relatively clear for 640D-F5 using the method shown in Table 6, 640D-F5 was not included in the following method optimization process.

The stacked chromatograms of 640D and 640D-F2 acquired at wavelength=210nm using the method shown in Table 7 was shown below in Figure 20.

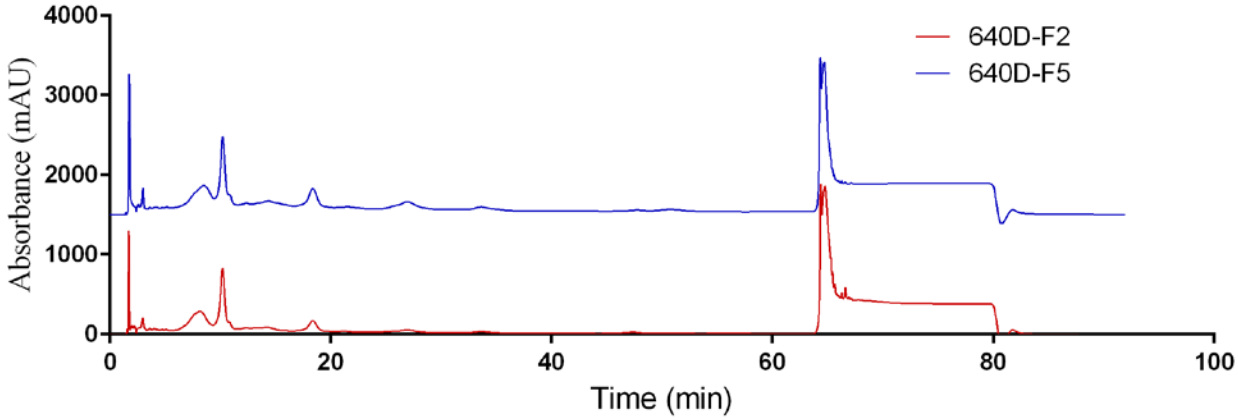

Figure 20. Stacked HPLC chromatograms of 640D and 640D-F2 at λ =210nm acquired by Agilent ZORBAX SB-Phenyl column and the method shown in Table 7.

Figure 20 indicates a much clearer separation of peaks compared to Figure 17. According to the appearance of peaks in Figure 19 and 20, both the method shown in Table 6 and the method shown in Table 7 improve the separation of peaks. Thus, these two methods were put together to generate a new method shown in Table 10 and Figure 21.

Table 10. Integrated HPLC method for 640D samples fractionated by XAD-2 resin column on a 4.6*150mm Agilent ZORBAX SB-Phenyl column

Solvent System	Sample injection volume (uL)	Time (min)	A (%)	B (%)	Flow Rate (mL/min)
A=0.1%formic acid in H_2O, B= 0.1% formic acid in methanol	10	13.50	98.0	2.0	1.00
		18.00	85.0	15.0	1.00
		48.00	85.0	15.0	1.00
		51.50	70.0	30.0	1.00
		62.00	45.0	55.0	1.00
		73.31	0.0	100.0	1.00
		95.81	0.0	100.0	1.00
		95.91	98.0	2.0	1.00
		109.36	98.0	2.0	1.00

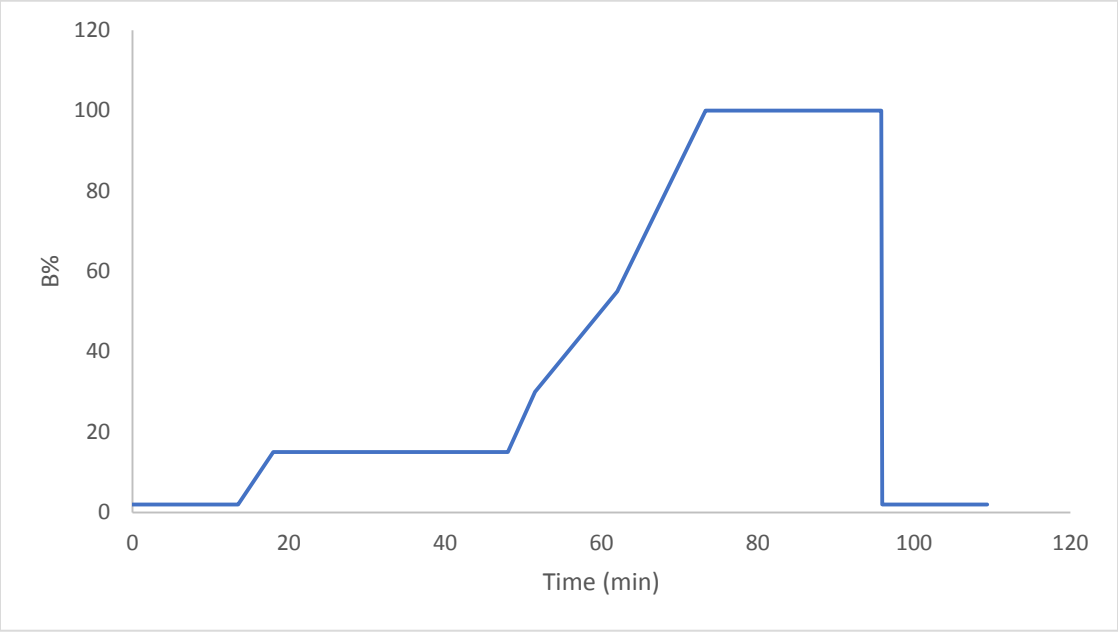

Figure 21. Solvent gradient diagram of the HPLC method shown in Table 8.

The chromatograms of 640D and 640D-F2 acquired by using the method shown in Table 9 were shown in Figure 22.

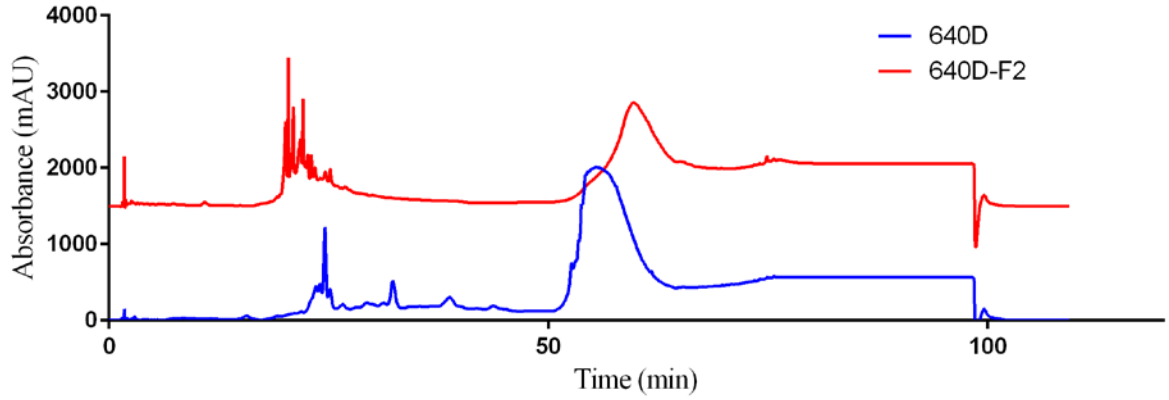

Figure 22. Stacked HPLC chromatograms of 60D and 640D-F2 acquired at λ =210nm by Agilent ZORBAX SB-Phenyl column and the method shown in Table 8.

With this integrated method, clear separation of majority of the peaks was achieved on 640D and 640D-F2 chromatograms except for the big wide peak retained between 52 and 60 minutes that might be composed of polymers of a single compound or chemicals of similar structures. Hence, this method was applied to the following liquid chromatography-mass spectroscopy (LC-MS) experiment for further investigation of the chemical composition of 640D.

4.3) Liquid Chromatography-Mass Spectroscopy Results and Putative Structure Analysis

Using the HPLC method provided in Table 8, the stacked chromatograms for parent sample 640, 640D and fraction 640D-F1~F5 acquired at wavelength=210nm were generated and shown in Figure 23.

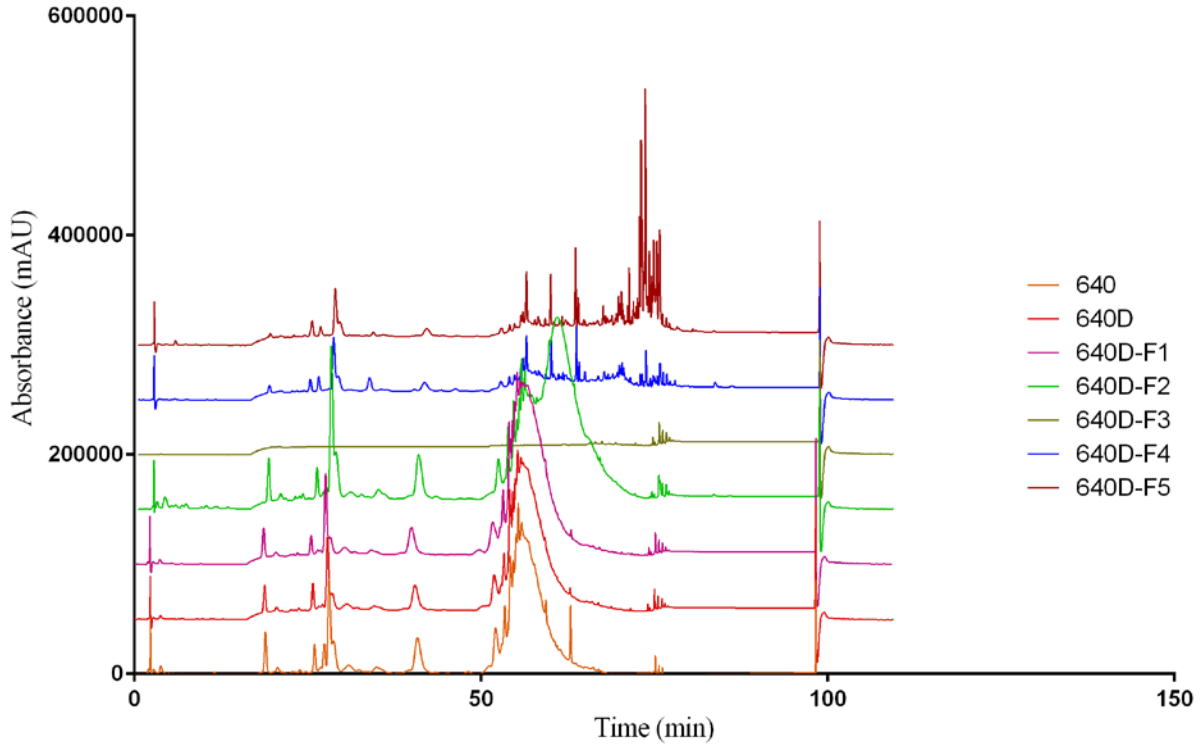

Figure 23. Stacked HPLC chromatograms of CQ-640, 640D and 640D-F1~F5 acquired at λ =210nm by Agilent ZORBAX SB-Phenyl column and the method shown in Table 8.

Using the Fourier-Transform Mass Spectroscopy (FTMS) technique, a negative mode and a positive mode mass spectrum were generated for the parent sample 640, 640D and each 640D fraction. These mass spectrums were shown in Figure 24-30. Since there was no absorbance after 100 minutes, those regions on the original mass spectrums were ignored and the spectrums were amplified on scale.

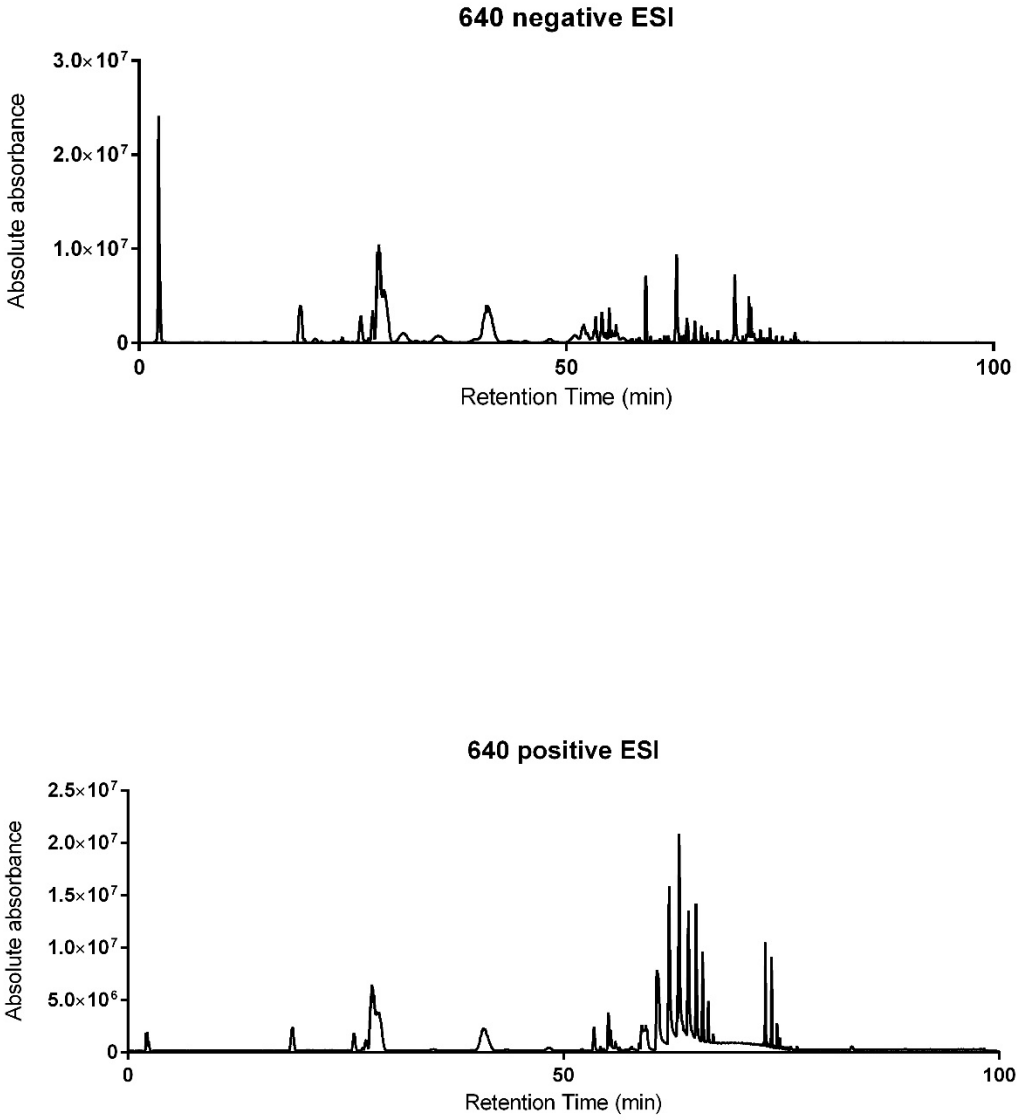

Figure 24. FTMS spectrum of Extract CQ-640

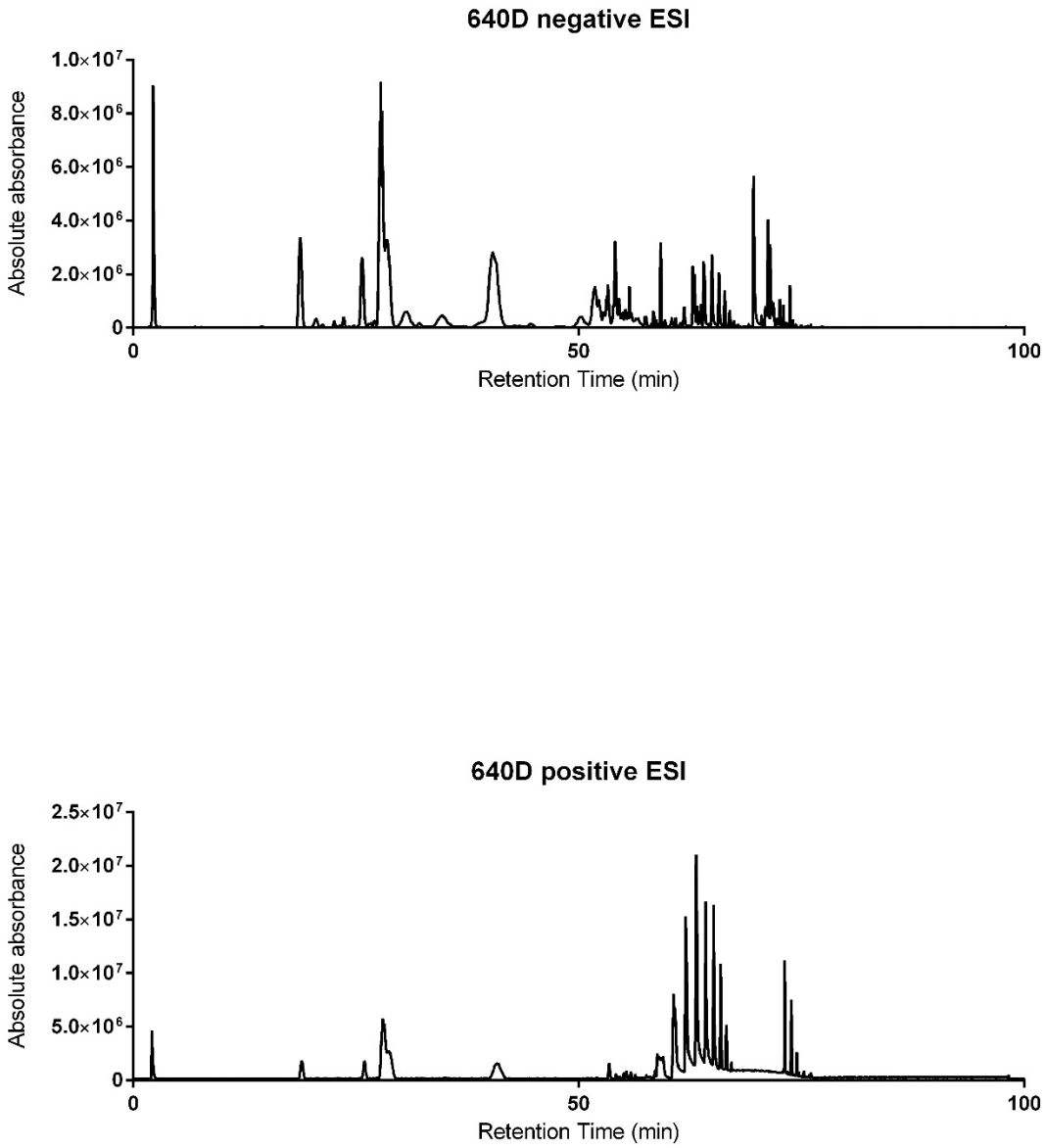

Figure 25. FTMS spectrum of 640D

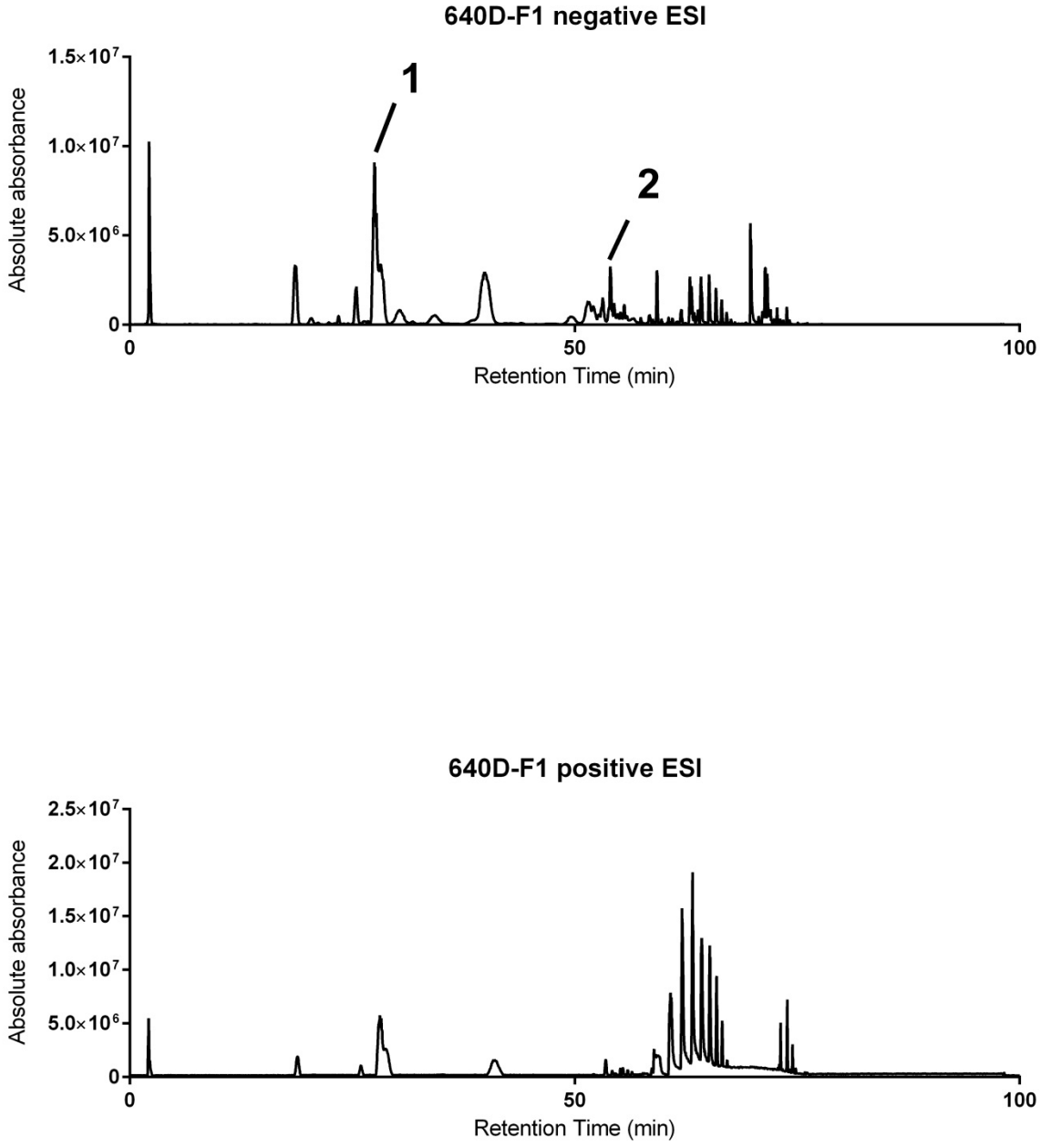

Figure 26. FTMS spectrum of 640D-F1

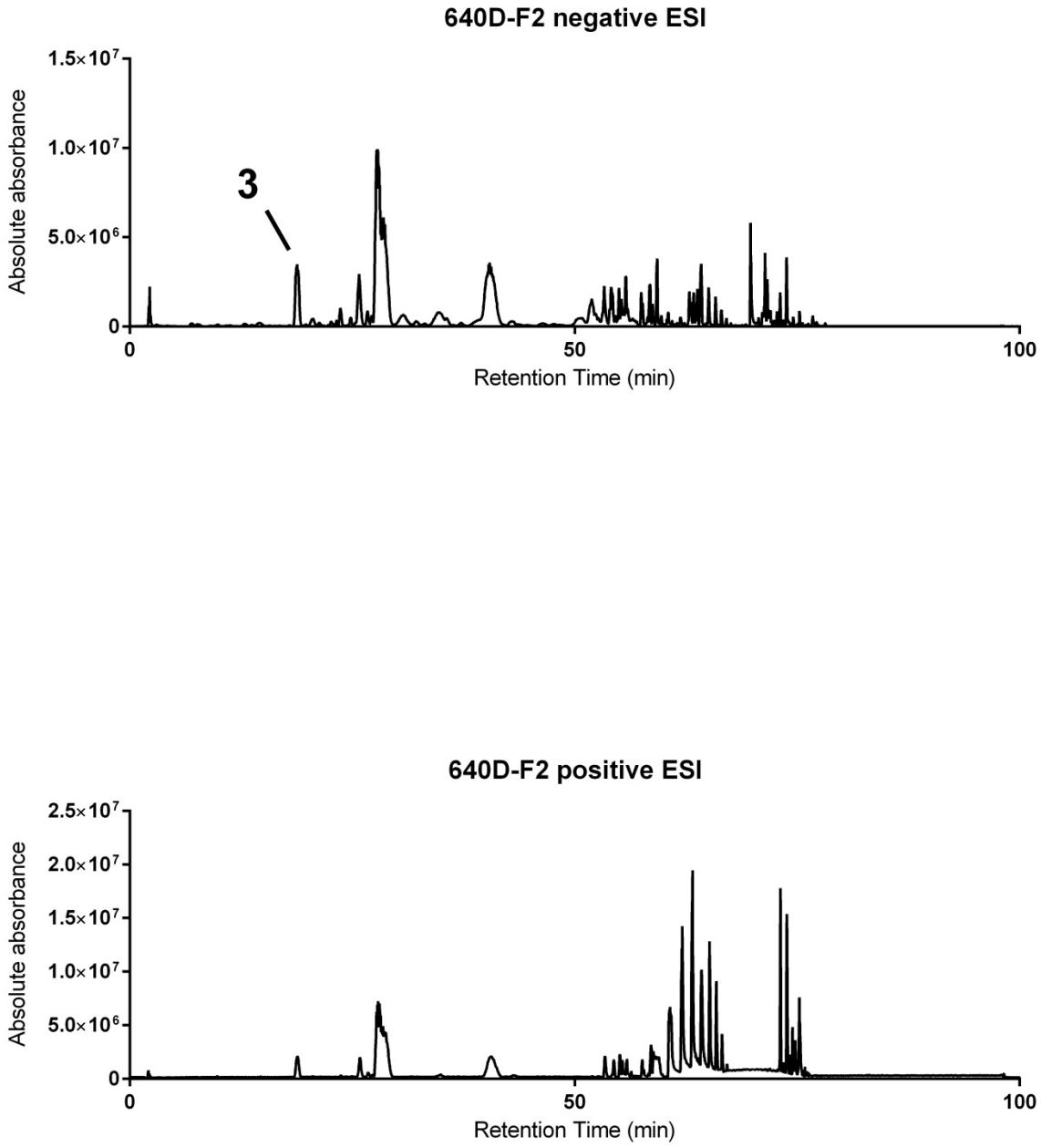

Figure 27. FTMS spectrum of 640D-F2

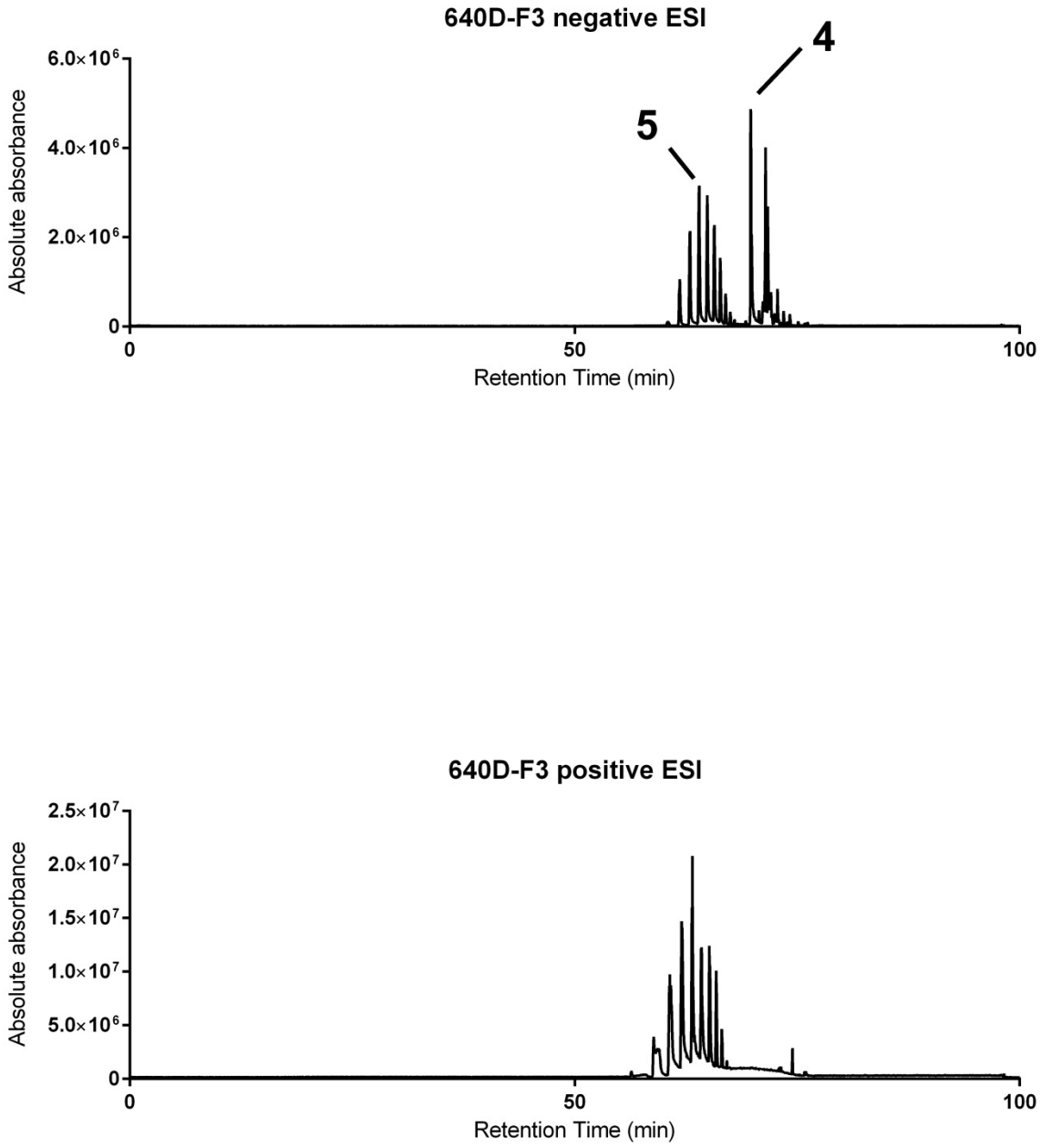

Figure 28. FTMS spectrum of 640D-F3

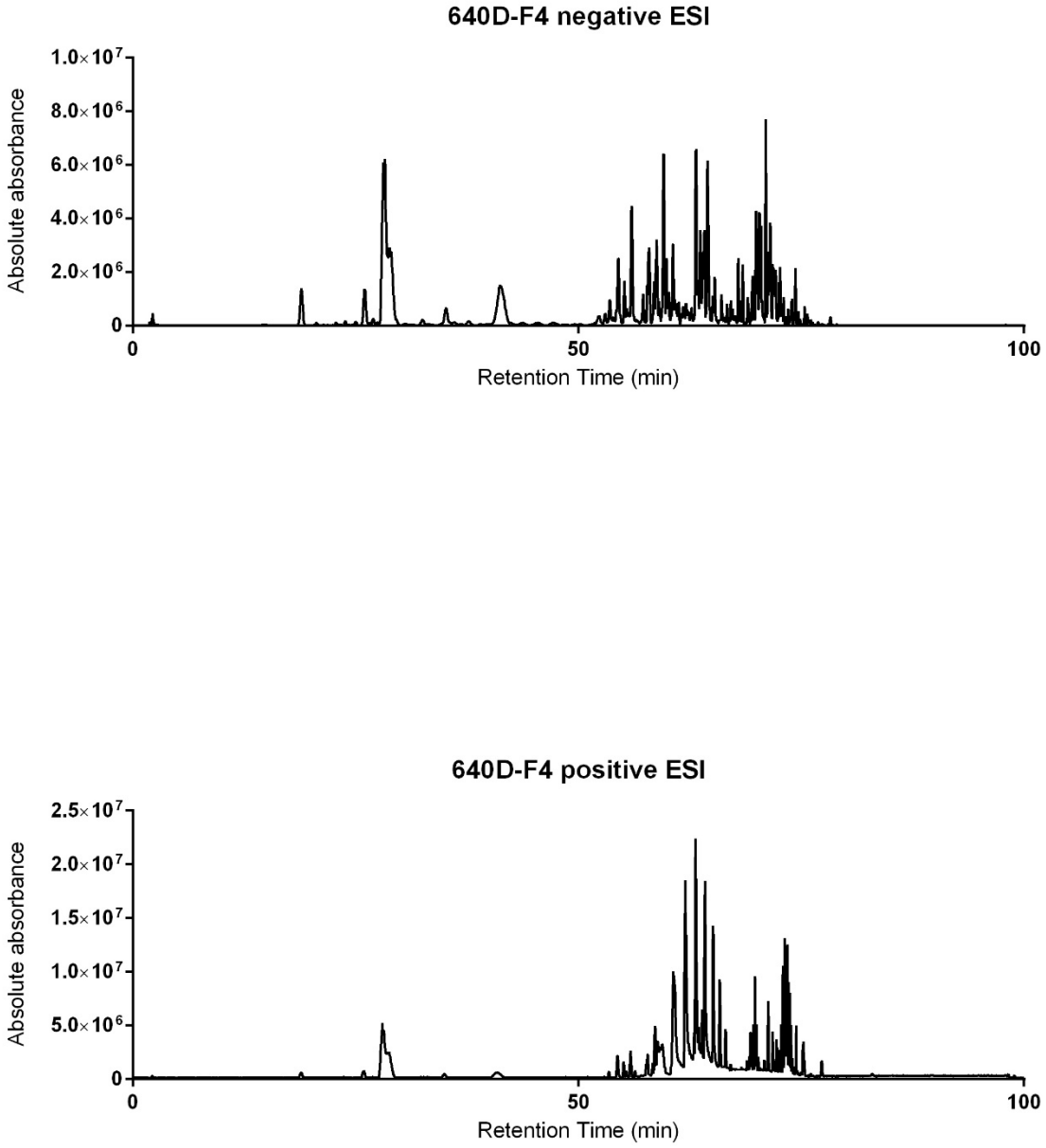

Figure 29. FTMS spectrum of 640D-F4

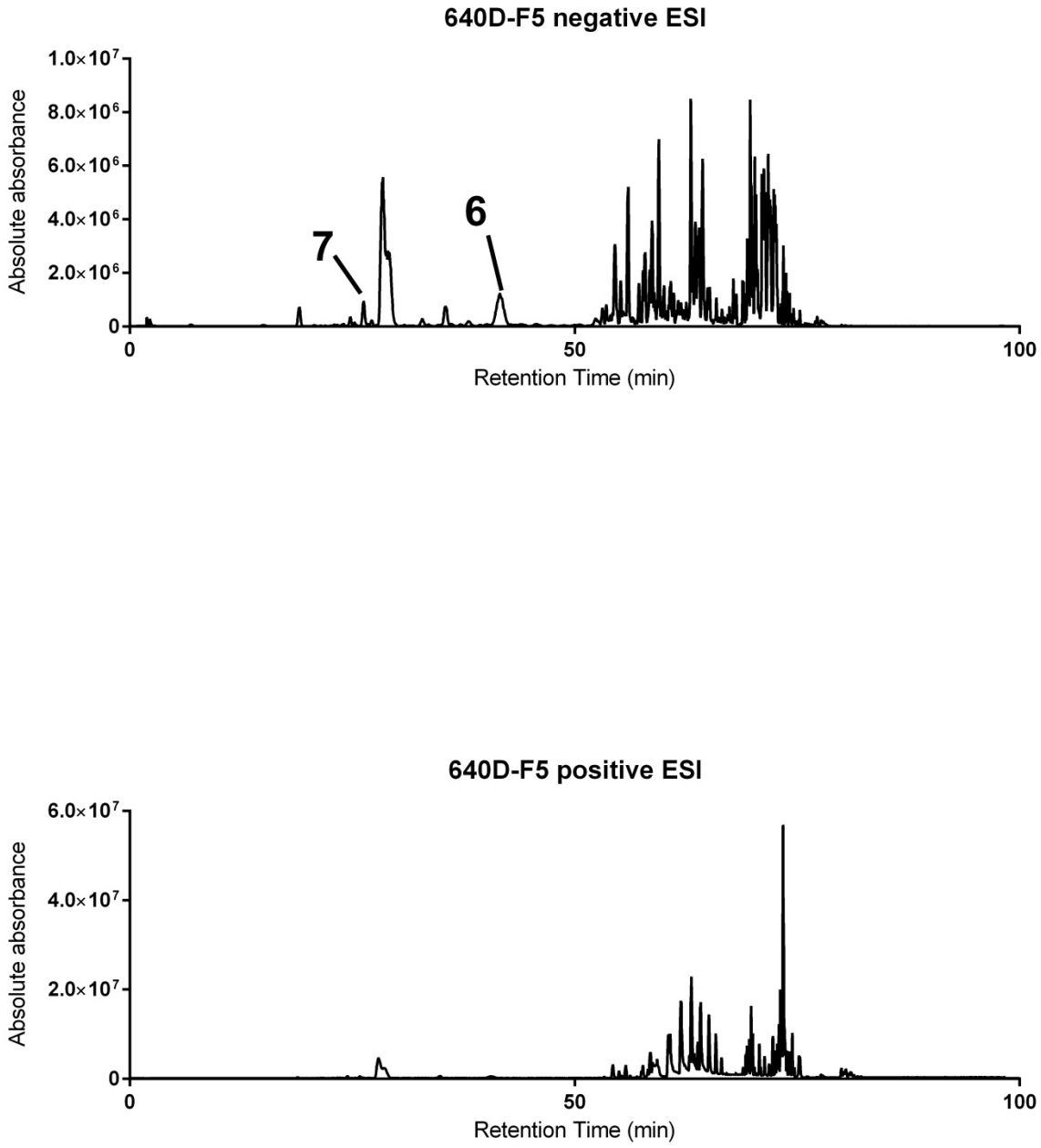

Figure 30. FTMS spectrum of 640D-F5

All the peaks in the mass spectrum were integrated and all the peaks with a % height higher than 1% were counted in the putative structure analysis. Due to time limit, not all the peaks were analyzed in this experiment. The following peaks were detected under the negative mode FTMS: peak 1 detected in the spectrum of 640D-F1 with a retention time of 27.49 minutes has a mass to charge (m/z) ratio of 577.1379 and the generated molecular formula is $C_{30}H_{25}O_{12}^-$ (Δ ppm =1.8), which matches up with the mass of procyanidin B4, (+)-procyanidin B2, (-)-procyanidin B3, (+)-procyanidin B1, procyanidin B8, proanthocyanidin B7, procyanidin B6, proanthocyanidin B5; peak 2 detected in the spectrum of 640D-F1 with a retention time of 54.01 minutes has a m/z ratio of 720.1610 and the generated molecular formula is $C_{25}H_{36}O_{24}^{2-}$ (Δ ppm =1.7), which has no match up with reported chemicals found in *Carya illinoensis* or *Carya tomentosa*; peak 3 detected in the spectrum of 640D-F2 with a retention time of 18.81 minutes has a m/z ratio of 575.1216 and the generated molecular formula is $C_{30}H_{23}O_{12}^-$ (Δ ppm =3.6), which matches up with the mass of (+)-proanthocyanidin A2; peak 4 detected in the spectrum of 640D-F3 with a retention time of 69.79 minutes has a m/z ratio of 553.2874 and the generated molecular formula is $C_{25}H_{45}O_{13}^-$ (Δ ppm =1.5), which has no match up with reported chemicals found in *Carya illinoensis* or *Carya tomentosa*; peak 5 detected in the spectrum of 640D-F3 with a retention time of 63.99 minutes has a m/z ratio of 635.3521 and the generated molecular formula is $C_{45}H_{47}O_3^-$ (Δ ppm =1.6), which has no match up with reported chemicals found in *Carya illinoensis* or *Carya tomentosa*; peak 6 detected in the spectrum of 640D-F5 with a retention time of 41.61 minutes has a m/z ratio of 865.1988 and the generated molecular formula is $C_{45}H_{37}O_{18}^-$ (Δ ppm =0.27), which matches up with the mass of procyanidin C2 and procyanidin C1; peak7 detected in the spectrum of 640D-F5 with a retention time of 26.27 minutes has a m/z ratio of 447.0953 and the generated molecular formula is $C_{21}H_{19}O_{11}^-$ (Δ ppm =2.0), which matches up with the mass of kaempferol 3-galactoside. The FTMS data and putative structural analysis results were shown in Table 11. The matched structures were shown in Figure 31 and 32.

Table 11. Putative structural analysis of 640D-F1~F5 mass spectrum

Peak #	Fraction	Retention Time (min)	Detected m/z (M-H)-	Candidate Formula (Δ ppm)	Putative Compound	Putative Compound Formula
1	1	27.49	577.1379	$C_{30}H_{25}O_{12}^-$(1.8)	Procyanidin B4, (+)-Procyanidin B2, (-)-Procyanidin B3, (+)-Procyanidin B1, Procyanidin B8, Proanthocyanidin B7, Procyanidin B6, Proanthocyanidin B5	$C_{30}H_{26}O_{12}$
2	1	54.01	720.1610	$C_{25}H_{36}O_{24}^{2-}$ (1.7)	no match	no match
3	2	18.81	575.1216	$C_{30}H_{23}O_{12}^-$(3.6)	(+)-Proanthocyanidin A2	$C_{30}H_{24}O_{12}$
4	3	69.79	553.2874	$C_{25}H_{45}O_{13}^-$ (1.5)	no match	no match
5	3	63.99	635.3521	$C_{45}H_{47}O_3^-$ (-1.6)	no match	no match
6	5	41.61	865.1988	$C_{45}H_{37}O_{18}^-$ (0.27)	Procyanidin C2, Procyanidin C1	$C_{45}H_{38}O_{18}$
7	5	26.27	447.0953	$C_{21}H_{19}O_{11}^-$ (2.0)	Kaempferol 3-galactoside	$C_{21}H_{20}O_{11}$

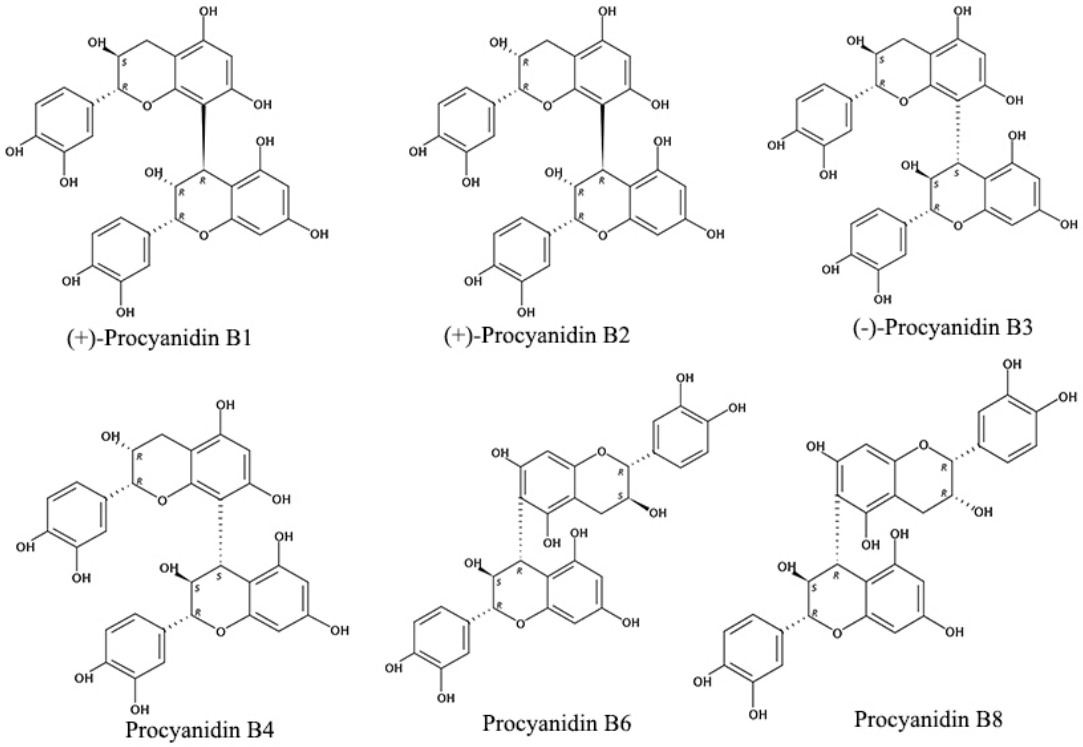

Figure 31. Chemical structures found in literature that match the FTMS data (1)

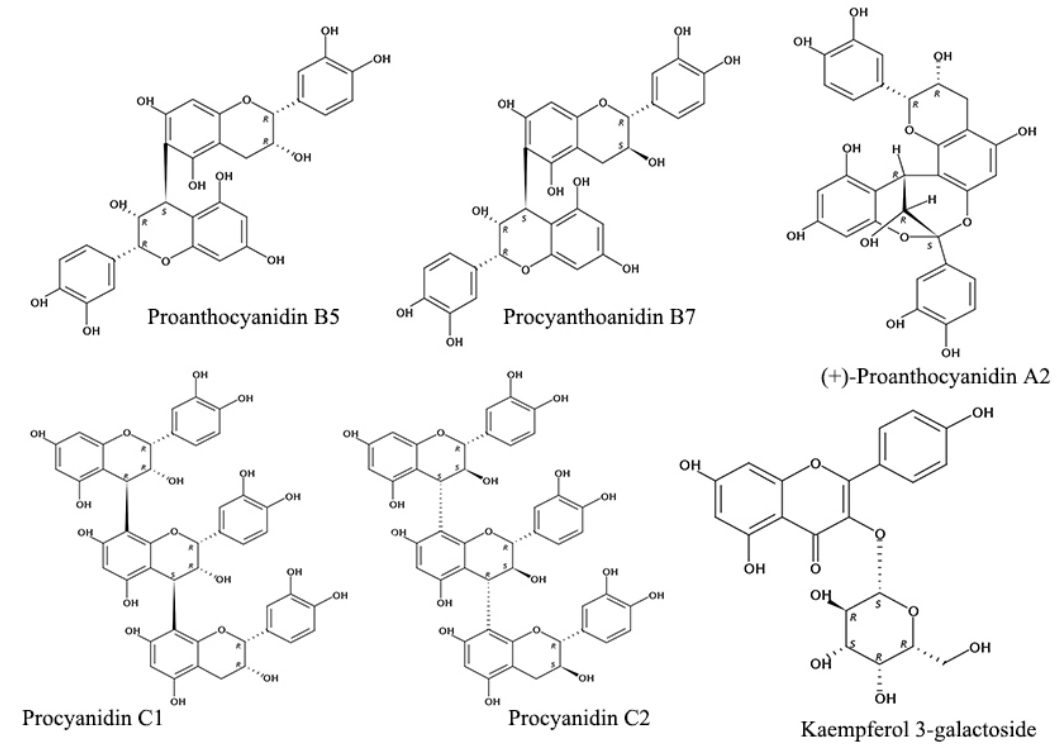

Figure 32. Chemical structures found in literature that match the FTMS data (2)

5) Conclusion

Overall, a fractionation method and a corresponding HPLC and LC-MS analysis method are generated for studying the chemical profile of *Carya tomentosa*. The fractionation process utilizes the Amberlite XAD-2 resin packing. The column could be prepared as following: mix the Amberlite XAD-2 resin with DI H_2O to make a slurry; add the slurry into a 130cm x1.5cm glass column; after the column is ¾ filled, backwash the column and flush the column with a pH=2 hydrochloric acid solution till the pH value of the eluate is the same as that of the eluent; Flush the column again with DI H_2O till the pH of the eluate IS approximately neutral. To fractionate 640D samples, dissolve 2.33 grams of 640D powder in DI H_2O and load the solution onto the column; add three column volumes of DI H_2O, then three column volumes of 1:1 MeOH: H_2O solution, and finally three column volumes of MeOH; collect fractions by the following scheme: first column volume as F0→ next three column volumes as F1→ next one column volume as F2→ next three column volumes as F3→ next one column volume as F4→ final three column volumes as F5. This fractionation method gave a total recovery yield of 93.41%. A 4.6*150mm Agilent ZORBAX SB-Phenyl column with the HPLC method shown in Table 8 was examined to be an appropriate approach for analyzing the chemical composition of the fractionated 640D samples. Using this method, a LC-MS study was conducted, and some putative structures were detected based on the mass data and literature search. These phytochemicals include procyanidin B4, (+)-procyanidin B2, (-)-procyanidin B3, (+)-procyanidin B1, procyanidin B8, proanthocyanidin B7, procyanidin B6, proanthocyanidin B5, (+)-Proanthocyanidin A2, procyanidin C2, procyanidin C1 and kaempferol 3-galactoside. The possible presence of procyanidins and proanthocyanidins in 640D-F1, F3 and F5 was in alignment with the observed dark color presence of those fractions. The putative structural analysis is also in alignment with the high contents of condensed tannins and flavonoids reported in chemical composition of *Carya illinoensis* and *Carya tomentosa*. However, it is also noticed that many peaks detected in FTMS spectrums do not match with previously reported structures. Interestingly, none of the

peaks in 640D-F3 match up with any previously reported chemicals found in *Carya illinoensis* and *Carya tomentosa.*

Future works would focus on identification of those unidentified peaks detected in FTMS spectrums, collection of pure compounds through preparatory level HPLC, structure elucidation through X-ray crystallography and nuclear magnetic spectroscopy (NMR) and conduction of anti-ZIKV bioassays on those identified compounds.

References

1. Leslie Collier, A. B., , Max Sussman, *Topley and Wilson's Microbiology and Microbial Infections*. Hodder Education Publishers: 1998; Vol. 1.
2. Zika Virus. https://www.cdc.gov/zika/about/index.html (accessed Dec 21).
3. Sirohi, D.; Chen, Z.; Sun, L.; Klose, T.; Pierson, T. C.; Rossmann, M. G.; Kuhn, R. J., The 3.8 A resolution cryo-EM structure of Zika virus. *Science* **2016,** *352* (6284), 467-70.
4. Wolford, R. W.; Schaefer, T. J., Zika Virus. In *StatPearls*, Treasure Island (FL), 2019.
5. Duffy, M. R.; Chen, T. H.; Hancock, W. T.; Powers, A. M.; Kool, J. L.; Lanciotti, R. S.; Pretrick, M.; Marfel, M.; Holzbauer, S.; Dubray, C.; Guillaumot, L.; Griggs, A.; Bel, M.; Lambert, A. J.; Laven, J.; Kosoy, O.; Panella, A.; Biggerstaff, B. J.; Fischer, M.; Hayes, E. B., Zika virus outbreak on Yap Island, Federated States of Micronesia. *N Engl J Med* **2009,** *360* (24), 2536-43.
6. Miles, T. Zika virus set to spread across Americas, spurring vaccine hunt. . https://www.reuters.com/article/us-health-zika-idUSKCN0V30U6 (accessed Dec 30).
7. Demain, A. L.; Fang, A., The natural functions of secondary metabolites. *Adv Biochem Eng Biotechnol* **2000,** *69*, 1-39.
8. Freeman, B., An Overview of Plant Defenses against Pathogens and Herbivores. *Plant Health Instructor* **2008,** *149*.
9. Hitmi, A.; Coudret, A.; Barthomeuf, C., The production of pyrethrins by plant cell and tissue cultures of Chrysanthemum cinerariaefolium and Tagetes species. *Crit Rev Biochem Mol Biol* **2000,** *35* (5), 317-37.
10. Armah, C. N.; Mackie, A. R.; Roy, C.; Price, K.; Osbourn, A. E.; Bowyer, P.; Ladha, S., The membrane-permeabilizing effect of avenacin A-1 involves the reorganization of bilayer cholesterol. *Biophysical journal* **1999,** *76* (1 Pt 1), 281-290.

11. Shukla, D.; Spear, P. G., Herpesviruses and heparan sulfate: an intimate relationship in aid of viral entry. *J Clin Invest* **2001,** *108* (4), 503-10.

12. Newman, D. J.; Cragg, G. M., Natural Products as Sources of New Drugs from 1981 to 2014. *Journal of Natural Products* **2016,** *79* (3), 629-661.

13. Horwitz, S. B., Taxol (paclitaxel): mechanisms of action. *Ann Oncol* **1994,** *5 Suppl 6*, S3-6.

14. Meshnick, S. R., Artemisinin antimalarials: mechanisms of action and resistance. *Med Trop (Mars)* **1998,** *58* (3 Suppl), 13-7.

15. Chakraborty, P., Herbal genomics as tools for dissecting new metabolic pathways of unexplored medicinal plants and drug discovery. *Biochim Open* **2018,** *6*, 9-16.

16. Tantaquidgeon, G., *A Study Of Delaware Indian Medicine Practice And Folk Beliefs*. Kessinger Publishing, LLC: 2010; p 108.

17. Wood, R., *The New Whole Foods Encyclopedia: A Comprehensive Resource for Healthy Eating*. Penguin Books: 2010.

18. de la Rosa, L. A.; Alvarez-Parrilla, E.; Shahidi, F., Phenolic compounds and antioxidant activity of kernels and shells of Mexican pecan (Carya illinoinensis). *J Agric Food Chem* **2011,** *59* (1), 152-62.

19. Diane L. McKay, M. E., C. Y. Oliver Chen, and Jeffrey B. Blumberg, A Pecan-Rich Diet Improves Cardiometabolic Risk Factors in Overweight and Obese Adults: A Randomized Controlled Trial. *Nutrients* **2018,** *10* (3), 339.

20. Katherine S. Carlos, Y. G. M. L. W., Phillip Greenspan, Ronald B. Pegg, Investigation of the antioxidant capacity and phenolic constituents of U.S. pecans. *Journal of Functional Foods* **2015,** *15*.

21. Cannell, R. J. P., *Natural Products Isolation*. 1 ed.; Humana Pr Inc: 1998.

22. Reginald H. Garrett, C. M. G., *Biochemistry*. 006 ed.; Cengage Learning: 2016.

23. Schendel, R. R.; Becker, A.; Tyl, C. E.; Bunzel, M., Isolation and characterization of feruloylated arabinoxylan oligosaccharides from the perennial cereal grain intermediate wheat grass (Thinopyrum intermedium). *Carbohydr Res* **2015,** *407*, 16-25.

24. Pettit, G. R.; Tang, Y.; Zhang, Q.; Bourne, G. T.; Arm, C. A.; Leet, J. E.; Knight, J. C.; Pettit, R. K.; Chapuis, J. C.; Doubek, D. L.; Ward, F. J.; Weber, C.; Hooper, J. N., Isolation and structures of axistatins 1-3 from the Republic of Palau marine sponge Agelas axifera Hentschel. *J Nat Prod* **2013,** *76* (3), 420-4.

25. Pedan, V.; Fischer, N.; Rohn, S., Extraction of cocoa proanthocyanidins and their fractionation by sequential centrifugal partition chromatography and gel permeation chromatography. *Anal Bioanal Chem* **2016,** *408* (21), 5905-5914.